European Journal of Medicinal Chemistry 207 (2020) 112761

Contents lists available at ScienceDirect

European Journal of Medicinal Chemistry

journal homepage: http://www.elsevier.com/locate/ejmech

Discovery of methoxy-naphthyl linked *N*-(1-benzylpiperidine) benzamide as a blood-brain permeable dual inhibitor of acetylcholinesterase and butyrylcholinesterase

Mohd Abdullaha [a, b], Vijay K. Nuthakki [a, b], Sandip B. Bharate [a, b, *]

[a] Medicinal Chemistry Division, CSIR-Indian Institute of Integrative Medicine, Canal Road, Jammu, 180001, India
[b] Academy of Scientific & Innovative Research, Ghaziabad, 201002, India

ARTICLE INFO

Article history:
Received 2 August 2020
Received in revised form
15 August 2020
Accepted 15 August 2020
Available online 28 August 2020

Keywords:
Alzheimer's disease
e-pharmacophore modeling
1-Benzylpiperidine benzamide
Acetylcholinesterase
Butyrylcholinesterase

ABSTRACT

The cholinesterase enzymes play a vital role in maintaining balanced levels of the neurotransmitter acetylcholine in the central nervous system. However, the overexpression of these enzymes results in hampered neurotransmission. Both the major forms of cholinesterase enzymes *viz*. acetylcholinesterase (AChE) and butyrylcholinesterase (BChE) play a crucial role in blocking neurotransmission; therefore, in recent years, a strategy of dual cholinesterase inhibition is being explored. Herein, we developed an energy-optimized *e*-pharmacophore hypothesis AHHPRR from AChE-donepezil complex and screened a set of 15 scaffolds that were designed imaginarily. The ligand with *N*-(1-benzylpyridinium) benzamide framework has shown the highest fitness and volume score, which was chosen for synthesis and validation. A series of pyridinium benzamides were synthesized and screened for cholinesterase inhibition that led to the identification of **7b**, a naphthalene containing *N*-(1-benzylpiperidine) benzamide as a potent dual AChE and BChE inhibitor with IC_{50} values of 0.176, and 0.47 μM, respectively. The kinetic study indicated that **7b** inhibits AChE in a non-competitive manner with *Ki* value of 0.21 μM, and BChE in a mixed-fashion with *Ki* of 0.15 μM. The observed mode of inhibition was corroborated with molecular docking studies. The MD simulation studies pointed out that both AChE and BChE undergo low conformational changes in complex with **7b**. The benzamide **7b** displayed high BBB permeability in PAMPA assay, which indicates its potential for further exploration in preclinical studies for Alzheimer's disease.

1. Introduction

The prevalence of Alzheimer's disease (AD) is rapidly increasing throughout the world, and has already affected more than 50 million people [1]. The cholinergic deficit is the dominant pathological symptom in the brains of AD patients, resulting in problems of memory, thinking, and behaviour [2,3]. The hydrolytic cleavage of acetylcholine by cholinesterase enzymes results in a cognitive impairment and memory deficits, which is associated with AD [4,5]. Therefore, the current treatment of AD (donepezil, galantamine, and rivastigmine) predominantly involves the up-regulation of the cholinergic system in the synaptic cleft by inhibiting cholinesterases. The human brain contains two types of cholinesterase enzymes *viz*. acetylcholinesterase (AChE) and butyrylcholinesterase (BChE) that share 65% of the amino acid sequence, and both possessing a deep hydrophobic active site gorge of 20 Å [6]. The difference in their structural features contributes to the substrate specificity. The substrate specificity difference is due to the variations in the amino acid sequence in the active site gorge [7–9]. The active site gorge of AChE is further divided into two subsites called peripheral anionic site (PAS) and catalytic anionic site (CAS) [10,11]. The PAS is located at the entrance of active-site gorge that allosterically regulates the functions of AChE, and studies have shown that PAS is involved in Aβ aggregation [12,13]. Butyrylcholinesterase (BChE), which is also called as pseudocholinesterase, is mainly found in the blood plasma and in a small quantity in the brain [14]. In the brain, BChE is predominantly present in the glial cells [15], and is involved in the cholinergic mediation [16]. With the advancement in the AD biology, the

* Corresponding author. Medicinal Chemistry Division, CSIR-Indian Institute of Integrative Medicine, Canal Road, Jammu, 180001, India.
E-mail addresses: sbharate@iiim.res.in, sandipbharate@gmail.com (S.B. Bharate).

https://doi.org/10.1016/j.ejmech.2020.112761
0223-5234/

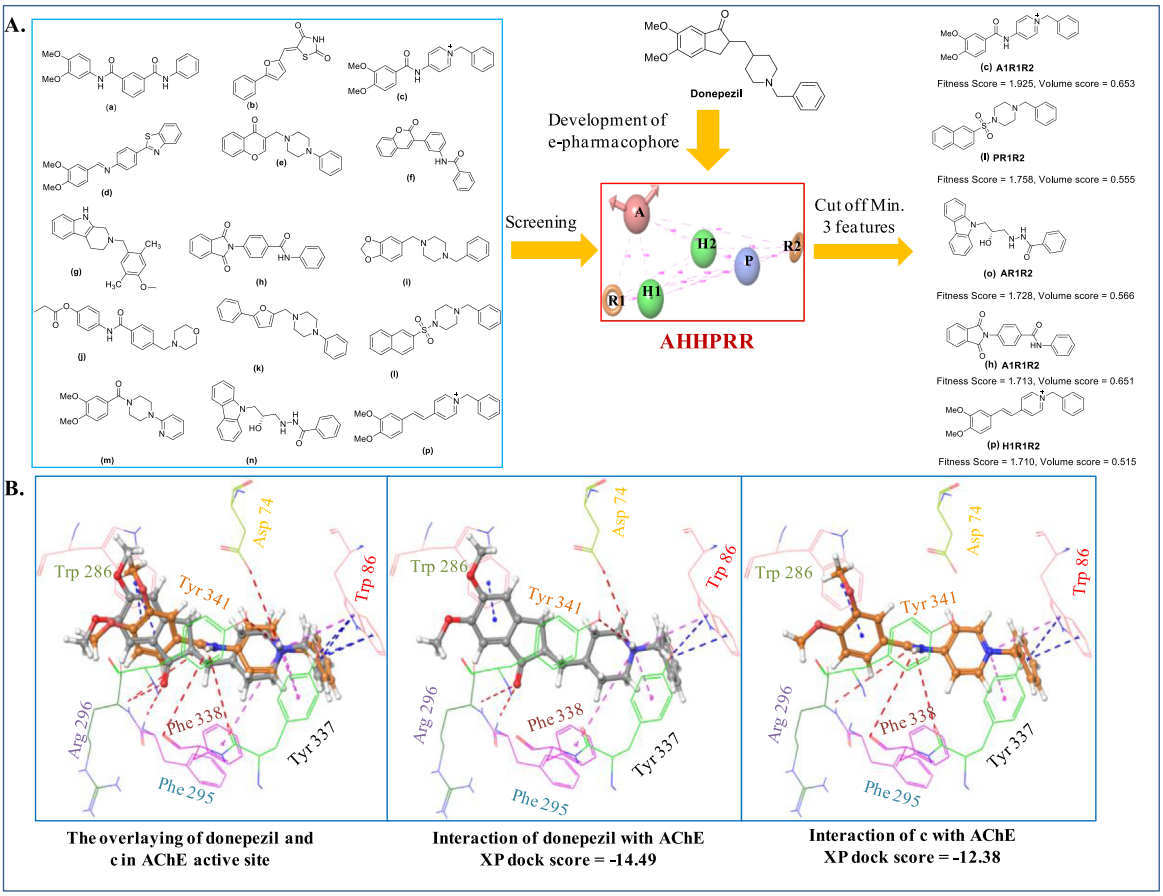

Fig. 1. **(A)** E-pharmacophore screening of designed compounds; **(B)** Interaction of donepezil and scaffold **c** with the active site of AChE.

increased activity of BChE has been detected in the hippocampus and temporal cortex parts of brain compared to its counterpart AChE, whose concentration is decreased in the specified regions [17,18]. Moreover, the activity of BChE is significantly increased with the age in AD brain, but no such correlation is observed in AChE enzyme [18]. Many studies have demonstrated that the inhibition of BChE is correlated with the improved memory in AD patients [17,19,20]. Initially, the inhibition of AChE was mainly taken into consideration to treat AD, however now several studies have shown the benefits of inhibiting both AChE and BChE parallelly in the treatment of AD [8]. Given the substantial involvement of BChE in the cholinergic regulation, and ultimately in the progression of AD, the dual inhibition is likely to provide additional advantage particularly in the long run [21,22]. Therefore, many potential dual inhibitors have been developed over the past decade [23–32].

Although numerous cholinesterase inhibitors are reported in the literature; however, the search for newer drug-like BBB-permeable scaffolds is a continuing process. The pharmacophore modeling is one of the tools commonly employed in designing potential drug-like inhibitors in drug discovery. Here, we applied an e-pharmacophore approach for design and the scaffold with highest fitness, volume, and dock scores was taken for synthesis, validation, and further lead optimization. Thus, we report the discovery of a naphthyl-linked piperidinyl benzamide as a dual cholinesterase inhibitor that has high BBB permeability.

Furthermore, the poor efficacy of single-targeted inhibitors in vivo has developed a pressing need towards development of multi-target-directed ligands (MTDLs) as potential therapeutics of AD.

2. Results and discussion

e-Pharmacophore based design. The e-pharmacophore based design approach has provided numerous lead structures in various therapeutic areas [33,34]. As our objective was to identify a new scaffold for dual inhibition of AChE and BChE inhibition, here we employed an e-pharmacophore based design approach. Donepezil was chosen for e-pharmacophore creation as it is an FDA approved drug, and along with AChE inhibition, it also possesses a moderate level of BChE inhibition (IC_{50} = 5.5 μM). The e-pharmacophore hypothesis AHHPRR was developed from the AChE-donepezil complex. The hypothesis is composed of one acceptor group (A), two hydrophobic groups (H), one positively charged group (P), and two aromatic rings (R) features. The hypothesis was validated using a database containing active and inactive set of ligands and was able to successfully differentiate active and inactive ligands. Then, the library of 15 scaffolds designed imaginarily was subjected to screening using this hypothesis. The scaffold **c** showed good fitness and volume score. The scaffold **c** was found to possess three features one acceptor and two rings (ARR) with fitness score and volume scores of 1.81, and 0.68. Scaffold **c** was found to superimpose with donepezil sharing various common interactions with the AChE. The phenyl moiety was found oriented towards the PAS region showing π-π stacking with TRP 286. The carbonyl group displayed H-bonding with TYR 124 and ARG 224 residues while the amine functionality displayed H-bonding interaction with TYR 337, and PHE 338 residues. Further, the nitrogen of pyridine formed a π-cation interaction with TYR 337 and also stacked with TRP 86. The benzyl ring was oriented towards CAS region showing π-π stacking

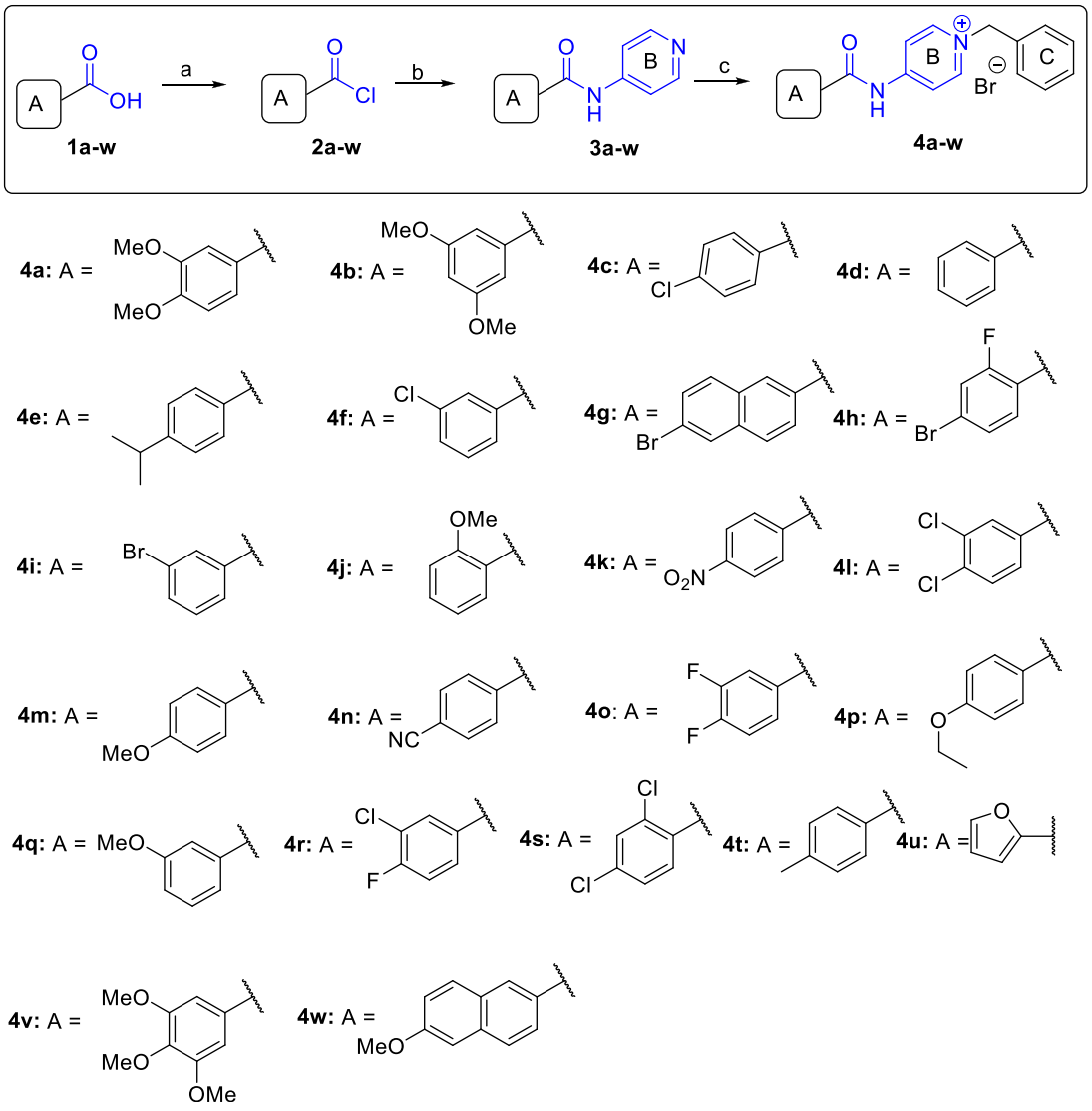

Fig. 2. Synthesis of pyridinium benzamides **4a-w**. Reagents and conditions: (a) oxalyl chloride, Dry THF, N_2, 0 °C, 2 h, >90%; (b) 4-aminopyridine, dry THF, 0 °C, 10 min, 75–90%; (c) ACN, benzyl bromide, 80 °C, 1 h, 87–95%.

with TRP 86. Based on the fitness, volume, and dock scores, the scaffold **c** was selected for its synthesis and further optimization. The e-pharmacophore based screening to identify a potential scaffold for cholinesterase inhibition is depicted in Fig. 1.

Synthesis and biological evaluation of benzamides 4a-w. The synthesis of pyridinium benzamides was started from commercially available aryl carboxylic acids **1a-w**. The treatment of aryl carboxylic acids **1a-w** with oxalyl chloride yielded corresponding acid chlorides **2a-w** in quantitative yields. The reaction of acid chlorides **2a-w** with 4-aminopyridine produced pyridinyl benzamides **3a-w** in 75-90% yield. Finally, refluxing the pyridine benzamides **3a-w** in the presence of benzyl bromide in acetonitrile resulted in the formation of pyridinium compounds **4a-w** in 87–95% yield. In this step, the product was obtained as a precipitate in the reaction mixture, in most of the cases. The obtained products were characterized by using NMR, mass, IR, and melting point analysis. The synthetic scheme for the preparation of products **4a-w** is depicted in Fig. 2.

The pyridinium benzamides **4a-w** were tested for inhibition of AChE and BChE at 1 and 10 μM using a modified Ellman assay [35]. All compounds displayed >90% inhibition of AChE at 10 μM. However at 1 μM, seven compounds **4a**, **4b**, **4k**, **4m**, **4n**, **4q** **4w** showed >70% inhibition of AChE. In the BChE inhibition assay, comparatively lesser inhibition was observed, with only two compounds showing significant inhibition at 1 μM. Compounds **4g** and **4w**, which bears a naphthyl ring (ring A), substantially inhibited BChE at 10 μM and >35% at 1 μM. Other compounds that showed >40% inhibition of BChE include **4e**, **4j**, **4p**, **4q**, and **4t**. It was interesting to note that the compounds bearing electron-withdrawing groups on the ring A, generally do not inhibit BChE (compounds **4h**, **4i**, **4k**, **4n**, **4o**, **4s**) or show only marginal inhibition (compounds **4c**, **4f**, **4l**). The significant difference in the BChE inhibition activity of compound **4g**, **4w**, and all other compounds could be because of the presence of bicyclic ring in **4g** and **4w**. The results of *in-vitro* inhibition of AChE and BChE by compounds **4a-w** are displayed in Table 1.

The IC_{50} values of best 7 compounds **4a**, **4b**, **4e**, **4g**, **4m**, **4n**, **4p,** and **4w** was then determined for AChE inhibition, and results are shown in Table 2. All 7 compounds displayed IC_{50} in the range of 0.2–1.4 μM. The most active compounds were **4b**, **4m, 4p,** and **4w**, showing IC_{50} values of 0.2–0.22 μM. One of the most potent AChE inhibitor (compound **4p**) and two most potent BChE inhibitors

Table 1
In-vitro inhibition of AChE and BChE by benzamides **4a-w**.

Entry	% Inhibition ±SEM			
	AChE[a]		BChE[b]	
	10 μM	1 μM	10 μM	1 μM
4a	91.45 ± 0.31	72.92 ± 0.24	na[c]	na[c]
4b	96.93 ± 0.39	86.82 ± 0.42	31.98 ± 1.44	na[c]
4c	91.36 ± 0.94	60.8 ± 0.14	13.16 ± 2.34	na[c]
4d	93.21 ± 0.71	61.01 ± 0.93	30.82 ± 1.4	na[c]
4e	95.70 ± 0.34	67.87 ± 0.92	48.48 ± 2.22	na[c]
4f	92.06 ± 0.13	63.31 ± 1.00	22.73 ± 1.57	na[c]
4g	99.29 ± 0.10	49.91 ± 1.15	86.83 ± 1.53	35.22 ± 1.92
4h	96.55 ± 0.51	62.45 ± 1.28	na[c]	na[c]
4i	94.90 ± 0.21	36.85 ± 0.46	na[c]	na[c]
4j	96.15 ± 0.36	68.17 ± 1.34	71.48 ± 0.70	na[c]
4k	96.27 ± 0.11	70.12 ± 0.99	na[c]	na[c]
4l	96.05 ± 0.46	51.45 ± 1.84	7.64 ± 0.23	na[c]
4m	94.95 ± 0.16	74.92 ± 0.24	6.65 ± 0.67	na[c]
4n	94.42 ± 0.4	78.71 ± 1.72	na[c]	na[c]
4o	90.13 ± 0.51	55.8 ± 0.70	na[c]	na[c]
4p	92.39 ± 0.36	62.36 ± 0.92	40.45 ± 0.13	na[c]
4q	97.08 ± 0.39	86.09 ± 0.41	42.30 ± 0.39	na[c]
4r	93.96 ± 0.05	66.67 ± 1.66	7.40 ± 0.26	na[c]
4s	92.01 ± 0.21	57.67 ± 0.83	na[c]	na[c]
4t	92.14 ± 0.20	58.94 ± 0.84	47.94 ± 0.28	na[c]
4u	90.41 ± 0.32	58.29 ± 1.75	8.57 ± 0.28	na[c]
4v	96.93 ± 0.39	86.82 ± 0.42	31.98 ± 1.44	na[c]
4w	96.36 ± 0.03	92.36 ± 0.94	88.83 ± 1.59	36.88 ± 1.29
Donepezil	99.42 ± 1.58	98.36 ± 1.52	67.85 ± 2.66	24.71 ± 2.29

[a] Percentage inhibition (mean ± SEM of three experiments) of AChE from *Electrophorus electricus*.
[b] Percentage inhibition (mean ± SEM of three experiments) of BChE from equine serum.
[c] Not active.

Table 2
IC_{50} values for inhibition of AChE, and BChE by selected compounds.

Entry	IC_{50} (μM ± SEM)[a]	
	AChE	BChE
4a	0.420 ± 0.022	nd
4b	0.202 ± 0.01	nd
4e	0.852 ± 0.171	nd
4g	1.442 ± 0.026	nd
4m	0.216 ± 0.018	nd
4n	0.469 ± 0.074	nd
4p	0.201 ± 0.006	12.65 ± 0.384
4w	0.218 ± 0.011	1.591 ± 0.021
Donepezil	0.049 ± 0.001	5.520 ± 1.05

nd is Not determined.
[a] The 50% inhibitory concentration of EeAChE, or eqBChE.

(compounds **4p**, **4w**) were then selected for IC_{50} determination against BChE. These two compounds have shown inhibition of BChE with IC_{50} values of 12.65, and 1.59 μM, respectively. The most promising compound from this series was the naphthyl ring containing compound **4w** that was found to be a dual inhibitor of AChE and BChE. The compound **4w** was ~3 fold more potent BChE inhibitor than donepezil.

Lead optimization studies for benzamide 4w. The significant difference in the BChE inhibition activity of compound **4g**, **4w,** and all other compounds, could be attributed to the presence of bicyclic ring in **4w** and **4g**. This initial screen provided us a naphthyl linked benzamide having an ability to inhibit both cholinesterases; however, the BChE inhibition activity requires further improvement. As depicted in Fig. 3, the compound **4w** was further optimized by substituting different electron-withdrawing and electron-donating groups on *N*-benzyl moiety (series A) and also incorporating a methyl linker (**4 ag**) and an ethyl linker (**4ah-4ap**) between amide and pyridine ring (series B). Initially, the naphthyl portion was kept constant, and modifications were imparted at other parts of the structure. In synthesis, the first step in all pyridinium based schemes involved activating the aromatic acids with EDC followed by coupling with amines in dry DCM at room temperature. Finally, refluxing pyridine amide intermediates with different benzyl halides/alkyl halides in ACN at 80 °C yielded corresponding pyridinium benzamides **4x-ap** in 80–95% yield (Fig. 3A–B). To probe the role of the positive charge on nitrogen, the pyridine ring was replaced with a piperidine ring (**7a-b**, Fig. 3C). Further, the naphthalene ring was also replaced with different biphenyls such as phenoxy phenyl, biphenyl, benzoyloxy phenyl, phenoxy benzyl (**4aq-at**, Fig. 3D–F) to explore the role of naphthalene that increases the potency against BChE. Furthermore, to check the role of benzyl ring in the activity, it was replaced with ethyl moiety (**4au**, Fig. 3G). A total of 26 new derivatives were further prepared as depicted in Fig. 3.

All compounds from Fig. 3 were tested at 1 μM against AChE and BChE. In the 6-methoxy-*N*-(pyridin-4-yl)-2-naphthamide series (Table 3), it was observed that the position of substituent on the pyridyl linked benzyl moiety has a significant effect on AChE as well as BChE inhibition. As a general trend, the 2-substituted derivatives (e.g., **4x, 4z, 4ac, 4af**) were superior over other substitutions. The comparison of this series of compounds with the parent lead **4w**, has indicated that only derivatives bearing substitution at ortho-position in benzyl ring have displayed similar level of AChE inhibition activity to that of **4w**. However, in case of BChE inhibition, all *ortho*-substituents do not display desirable level of BChE inhibition, with only 2-halo substituted compounds (e.g. **4z**, **4ac**) possess same level of BChE inhibition. The replacement of benzyl moiety with alkyl (e.g., **4au**) has resulted in drastic reduction in cholinesterase inhibition activity. This indicated that the benzyl moiety is essential for interaction at the catalytic anionic site of the AChE. Though few compounds from this series (Table 3) displayed similar level of activity profile to that of **4w**, but none displayed superior activity.

Another series of compounds '6-methoxy-*N*-(pyridin-4-yl-alkyl)-2-naphthamide **4 ag-ap'** (Table 4) was superior over **4x-4af** series (Table 3) with respect to dual inhibition. In this series, a "small alkyl linker" is placed between pyridyl moiety and amide linked naphthyl unit. This extra linker positively impacted the cholinesterase inhibition activity. The ethylene linker (**4ah**) was significantly superior to methylene linker (**4 ag**). Among the ethylene linker containing compounds, the substitution on *N*-benzyl was varied, where the 2-substitution was superior over other positions. Though there was somewhat low AChE inhibition in this series, however several compounds (**4ah**, **4aj**, **4ao**) have displayed superior inhibition of BChE than benzamide **4w**. This series has provided critical information that placing a small $-CH_2CH_2-$ linker between naphthylamide and pyridine ring imparts significant positive impact on potency. This additional spacer might be probably helping the compound to occupy the active site gorge perfectly, and helping it to interact with all key residues of both the active sites.

Next, when the pyridinium moiety of the first-stage lead compound **4w** was replaced with piperidine (compound **7a**), the cholinesterase inhibition activity was completely lost (7.7 and 1.8% inhibition at 1 μM) (Table 5). However, interestingly with simply an introduction of a ethylene linker between piperidine ring and naphthyl amide moiety (compound **7b**, Table 5) has resulted in the gain of activity against both cholinesterases. In fact, compound **7b**, though it does not bear quaternary nitrogen, still displayed the same level of AChE inhibition, and superior BChE inhibition compared to **4w**. Finally, we also explored the possibility of replacing the naphthyl moiety from **4w** with other biphenyl rings. The replacement of naphthyl with phenoxy-phenyl, biphenyl,

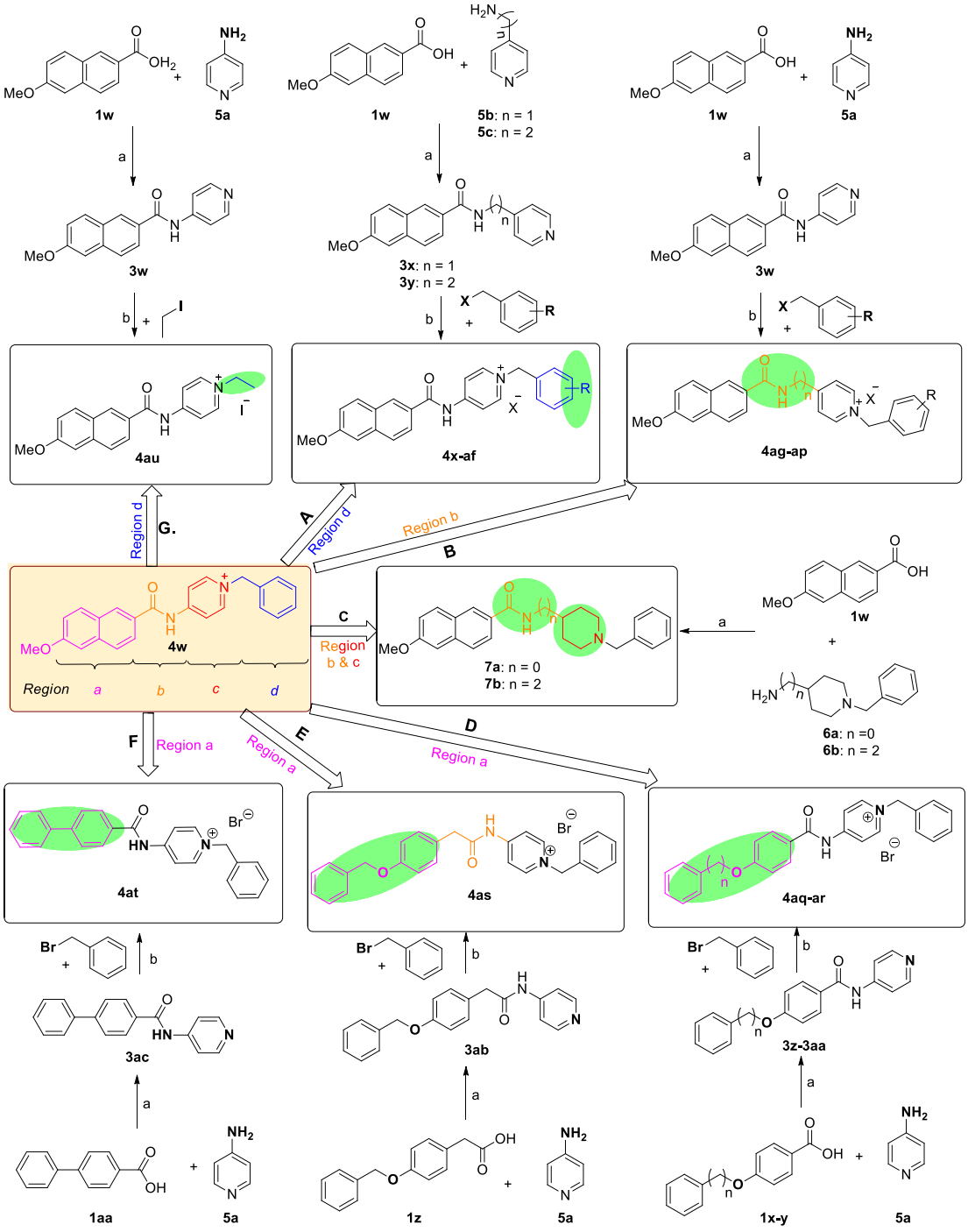

Fig. 3. Lead optimization studies for naphthyl linked benzamide derivative **4w**. Synthesis of naphthyl substituted pyridinium benzamides **4x-ap, 7a-b, 4aq-at, 4au**. Reagents and conditions: (a) EDC.HCl, Et_3N, Dry DCM, N_2, rt, 3 h, 77-91%; (b) ACN, substituted benzyl halides/alkyl halides, 80 °C, 1 h, 80–95%.

benzoyloxy-phenyl, phenoxy-benzyl (**4aq-at**) has resulted in loss of activity (Table 6), indicating that naphthalene ring is essential for dual cholinetserase inhibition.

The compounds showing inhibition >50% against AChE and BChE were subjected for IC_{50} determination (Table 7). Compounds **4ah, 4aj,** and **7b** were found to possess dual cholinesterase inhibition activity with IC_{50} values less than 1 μM for both enzymes. Though compounds **4ac**, **4ad**, and **4am** displayed potent inhibition of AChE (IC_{50} < 0.3 μM); however, their IC_{50} for BChE inhibition was >1 μM; therefore, these compounds were not investigated further.

The BBB permeability is the most vital parameter in CNS drug discovery. Therefore, two best compounds from Table 7 were selected for the BBB permeability analysis. A parallel artificial membrane permeation assay for BBB (PAMPA-BBB) was used to screen the permeability potential of **4ah**, and **7b**. The assay was validated by comparing the experimental and reported permeability values of three standards, including donepezil with higher permeability, carbamazepine having moderate permeability, and theophylline with low permeability. The P_e value of $>3.3 \times 10^{-6}$ cm/s is considered as BBB permeable [36,37]. Thus, the

Table 3
In-vitro inhibition of AChE and BChE by 6-methoxy-*N*-(pyridin-4-yl)-2-naphthamide series **4x-af, 4au**.

Entry	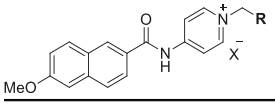		% inhibition ± SD (@ 1 μM)	
	R	X	AChE	BChE
4w	-Ph	Br	92.36 ± 0.94	36.88 ± 1.29
4x	-Ph (2-Me)	Br	88.59 ± 0.79	20.97 ± 0.93
4y	-Ph (4-OMe)	Cl	48.63 ± 0.79	7.94 ± 0.49
4z	-Ph (2-Cl)	Cl	91.67 ± 0.36	35.21 ± 0.49
4aa	-Ph (3-Cl)	Cl	18.05 ± 4.63	13.39 ± 8.56
4ab	-Ph (4-Cl)	Cl	67.30 ± 0.69	4.27 ± 1.39
4ac	-Ph (2-F)	Br	90.68 ± 0.66	33.24 ± 1.19
4ad	-Ph (4-F)	Cl	91.46 ± 0.49	35.56 ± 8.86
4ae	-Ph (2-NO_2)	Br	78.04 ± 4.22	10.85 ± 6.35
4af	-Ph (4-NO_2)	Br	49.27 ± 2.7	8.470 ± 0.43
4au	-CH_3	I	43.85 ± 9.97	22.39 ± 1.64
Donepezil	_	_	98.36 ± 1.52	24.71 ± 2.29

compound **7b** with permeability (P_e) value of 6.9 × 10^{-6} cm/s falls in the category of high BBB permeability. However, the other pyridinium-based compound **4ah** has low P_e value (1.3 × 10^{-6} cm/s), indicating its low BBB permeability. Thus, compound **7b**, possessing dual cholinesterase inhibition with IC_{50} values less than 0.5 μM (for both cholinesterases) and ability to cross BBB, was chosen for further studies. The compound **7b** was also checked for its inhibitory activity against human recombinant human AChE and was found to have an IC_{50} value of 0.17 μM.

Enzyme kinetic analysis for dual cholinetserase inhibitor 7b. In order to determine the type of hAChE and eqBChE inhibition by compound **7b**, we performed kinetic analyses using different concentrations of substrate (0.06 mM−1 mM) and inhibitor (0.015 μM−0.5 μM) and evaluated the results using Lineweaver-Burk double reciprocal (LB) plot (Fig. 4). LB plot was generated by plotting the reciprocal enzyme velocity (1/V) against reciprocal of substrate concentration (1/[S]) and was used to determine the mode of inhibition of the enzyme by the compound **7b**. From the graph, it was found that the increase in the inhibitor concentration results in a decrease in the V_{max} leaving the K_m value constant, indicating that the compound **7b** is a non-competitive inhibitor of AChE. Further, the slopes of the lines of the LB plot were plotted against the inhibitor concentration to determine the inhibition rate constant (*Ki*) for the enzyme-inhibitor complex, in which the value of the X-axis intercept is the *Ki*. From the graph, *Ki* was found to be 0.21 μM for hAChE. The LB plot constructed for eqBChE has shown that with an increase in the inhibitor concentration has led to a decrease in the V_{max} and an increase in K_m value, indicating that the compound **7b** is a mixed inhibitor of BChE. The replot of slopes of the LB plot against inhibitor concentration has been constructed to determine the *Ki*, which was found to be 0.15 μM for eqBChE.

To further investigate the multi-targeted nature of the identified dual AChE/BChE inhibitor, its ability to inhibit Aβ-aggregation was studied. Following thioflavin-T based fluorometric assay, the inhibitory activity of **7b** was determined against self-induced Aβ42 aggregation. Compound **7b** has shown Aβ42 anti-aggregating activity of 25% at 10 μM.

Molecular docking and MD simulation of 7b with AChE and BChE. To further understand the observed non-competitive and mixed-type of inhibition, the docking studies were performed for **7b** with human AChE (PDB: 4EY7) [38] and human BChE (PDB: 6EP4) [39] using Glide module of the Schrodinger molecular modeling software. The study demonstrated that the compound **7b** accommodates in the active site gorge interacting with the amino acid residues of both PAS and CAS of both enzymes (Fig. 5A−D). The naphthalene moiety of **7b** orients towards the peripheral site and its *N*-benzyl group towards the catalytic site of the AChE active site gorge. The close packing of the molecule inside the active site gorge

Table 4
In-vitro inhibition of AChE and BChE by 6-methoxy-*N*-(pyridin-4-yl-alkyl)-2-naphthamides **4 ag-ap**.

Entry	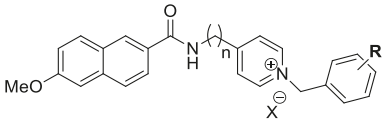			% inhibition ± SD (@ 1 μM)	
	n	R	X	AChE	BChE
4w	0	H	Br	92.36 ± 0.94	36.88 ± 1.29
4ag	1	H	Br	48.33 ± 2.78	2.41 ± 1.31
4ah	2	H	Br	78.93 ± 1.37	53.25 ± 1.55
4ai	2	2-Me	Br	61 ± 1.41	25.80 ± 0.493
4aj	2	2-Cl	Cl	78.69 ± 1.28	54.17 ± 2.12
4ak	2	3-Cl	Cl	69.89 ± 1.08	33.40 ± 2.00
4al	2	4-Cl	Cl	2.42 ± 8.07	19.35 ± 2.13
4am	2	2-F	Br	77.72 ± 0.23	29.74 ± 2.51
4an	2	4-F	Cl	66.35 ± 4.25	20.44 ± 1.58
4ao	2	2-NO_2	Br	46.58 ± 1.00	47.75 ± 2.15
4ap	2	4-NO_2	Br	6.33 ± 7.68	14.01 ± 4.32
Donepezil	_	_	_	98.36 ± 1.52	24.71 ± 2.29

Table 5
In-vitro inhibition of AChE and BChE by *N*-(1-benzylpiperidin-4-yl)-6-methoxy-2-naphthamides **7a-b**.

Entry	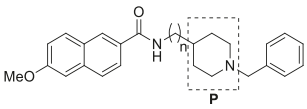	% inhibition ± SD (@ 1 μM)	
	n	AChE	BChE
4w	P = pyridinium, n = 0	92.36 ± 0.94	36.88 ± 1.29
7a	0	7.70 ± 5.59	1.77 ± 1.21
7b	2	**80.02 ± 1.10**	**60.98 ± 0.31**
Donepezil	_	98.36 ± 1.52	24.71 ± 2.29

Table 6
In-vitro inhibition of AChE and BChE by phenoxy phenyl, biphenyl, benzoyloxy phenyl, phenoxy benzyl substituted benzamides **4aq-at**.

Entry	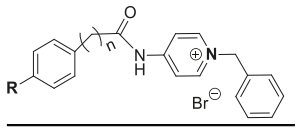		% inhibition ± SD (@ 1 μM)	
	R	n	AChE	BChE
4aq	-OBn	0	87.56 ± 0.51	12.74 ± 1.83
4ar	-OPh	0	34.21 ± 0.99	23.19 ± 5.06
4as	-OBn	1	6.16 ± 3.10	7.94 ± 0.49
4at	-Ph	0	60.07 ± 1.14	33.29 ± 1.35
Donepezil	_	_	98.36 ± 1.52	24.71 ± 2.29

Table 7
IC_{50} values for inhibition of EeAChE and eqBChE by selected naphthyl series of compounds.

Entry	IC_{50} (μM) ± SD	
	AChE	BChE
4x	0.435 ± 0.09	>1
4z	0.34 ± 0.04	>1
4 ab	0.9 ± 0.03	>1
4ac	0.21 ± 0.00	>1
4ad	0.21 ± 0.00	>1
4ae	0.48 ± 0.01	>1
4ah	**0.77 ± 0.07**	**0.68 ± 0.04**
4ai	1.08 ± 0.06	>1
4aj	0.50 ± 0.04	0.83 ± 0.04
4ak	0.61 ± 0.02	>1
4am	0.28 ± 0.04	>1
4an	0.74 ± 0.06	>1
4ao	0.28 ± 0.04	>1
4ap	0.74 ± 0.06	>1
7b	**0.41 ± 0.09**	**0.47 ± 0.01**
4aq	0.36 ± 0.03	>1
4 at	0.77 ± 0.03	>1
Donepezil	0.035 ± 0.023	5.25 ± 0.23

was observed by virtue of its various types of interactions such as H-bonding, π-π stacking, and π-cation interactions with residues of active site gorge. Further, it attains a position wherein carbonyl moiety establishes H-bonding with the Phe 295 and Arg 296 and −NH of amide forming a H-bonding with Asp 74 at the lining of the gorge. In the CAS region of active site gorge, the piperidine nitrogen has reproduced the cation-π interaction with Tyr 337 residue. The piperidine nitrogen also display cation-π interaction with Trp 86 of CAS. The *N*-benzyl ring and naphthalene moiety show π-π interaction with Trp 86, and Trp 286 residues, respectively indicating that the compound **7b** has ability to interact with both sites of the AChE active site gorge. Additionally, the NH of amide linker show H-bonding with Asp 74, which is present at the lining of the gorge. The strong interactions of **7b** with PAS could be attributed to its non-competitive mode of inhibition as observed in kinetic studies. Further, the docking investigation was also carried of **7b** with BChE. The NH of amide moiety was found engaged in H-bonding interaction with Asp 70, and nitrogen of piperidine display a cation-π interaction with Trp 82, and benzyl attains a position to stack with the Trp 82. The surface view (Fig. 5C) of BChE with **7b** depicts that the molecule bends in a U-shaped format because of the available space within the cavity. The interaction of **7b** with PAS in both cases corroborates with the kinetic analysis results.

The MD simulation studies were carried out for the most potent compound **7b** of the series with the targeted enzymes (AChE and BChE) over a period of 10 ns (Fig. 6). In the course of this study, RMSD of the protein backbone C-α atoms and individual inhibitor was recorded that was found to be in a range between 2 and 2.5, reflecting the stability of the protein-ligand complex. Further, the RMSF in the individual amino acid side chain was below 3 Å signifying conformational changes to a low degree in the protein during entire MD simulations. The reliability of MD simulation was also advocated by the constant temperature, pressure, volume, and potential energy during the whole course of time. The final frame analysis has indicated that **7b** occupies both the CAS and PAS regions of AChE during MD simulation time. In the PAS region, the contact between Trp 286 and naphthalene moiety was retained for >80% of the total simulation time. At the same time, the Phe 295 reproduced the H-bonding interaction with the carbonyl of the amide that was conserved throughout the simulation time. Further, the H-bonding interaction between Asp 74 and amine of piperidine was retained during the entire course of simulation time. Trp 86 was found engaged in a π-cation, and π-π stacking interactions with an amine of piperidine and *N*-benzyl moiety, respectively which were also conserved throughout the simulation time. At the same time, contacts between Tyr 341 and amine of piperidine persisted for>80% of the total simulation time. Further, in the case of BChE, the RMSD value was found below 2.5 Å, indicating the stability of the protein-ligand complex during a simulation. BChE also experienced a low degree of conformation as the value of RMSF was below 1.5. In addition, the interactions of **7b** with Trp 82 and Tyr 332 of BChE were also conserved throughout the simulation time.

3. Conclusion

In summary, the new scaffold predicted *via* e-pharmacophore modeling was validated experimentally *via* synthesizing a total of 49 compounds. This effort has resulted in the identification of a naphthyl linked benzylpiperidine-benzamide **7b** as a BBB permeable dual inhibitor of AChE and BChE (IC_{50} values of 0.17 and 0.47 μM). It inhibited AChE in a non-competitive fashion (*Ki* value of 0.1 μM) and BChE *via* a mixed-type of inhibition (*Ki* of 0.15 μM).

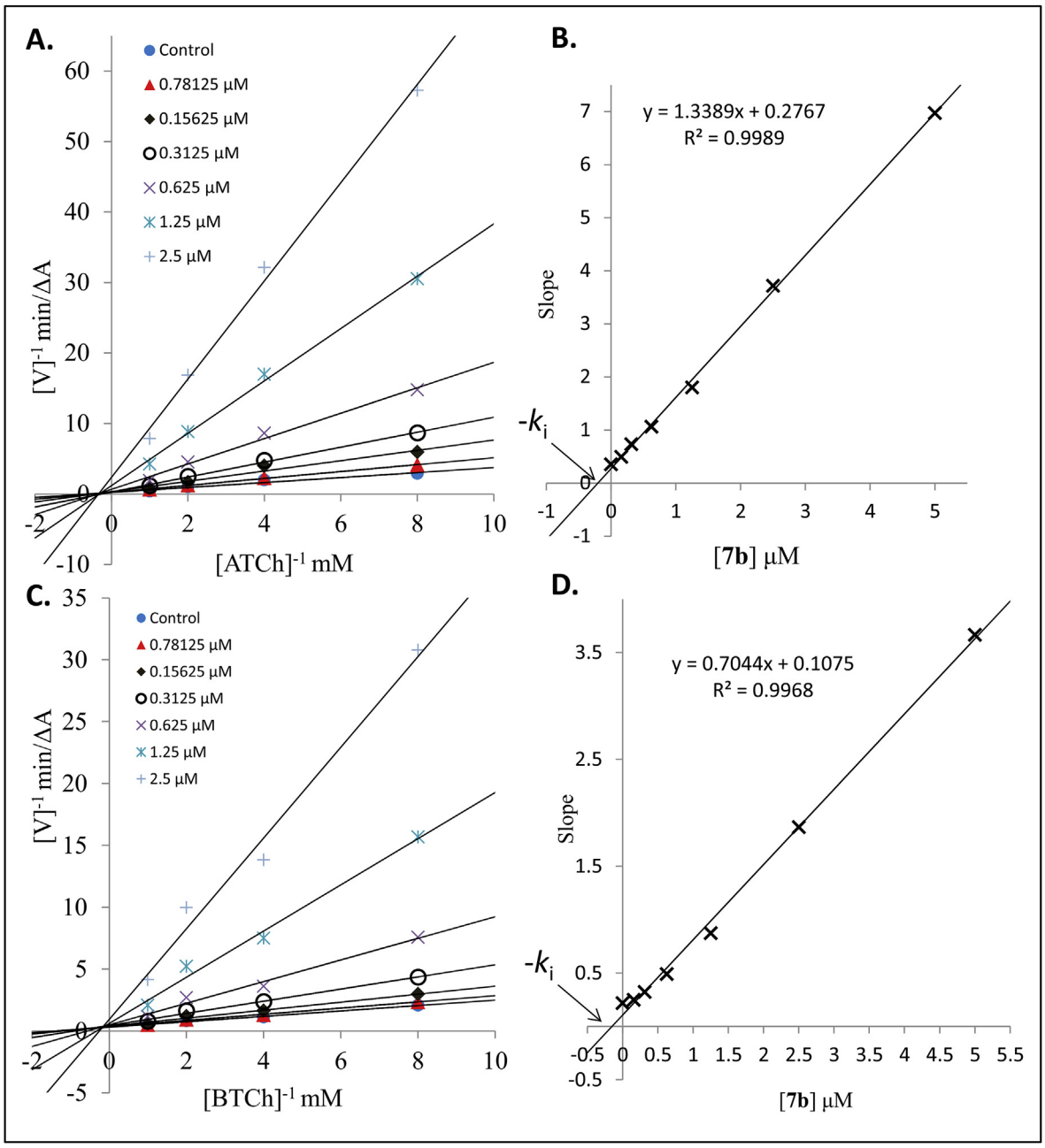

Fig. 4. Enzyme kinetics of **7b** with AChE and BChE. (A) LB plot for the inhibition of hAChE by **7b** (B) replot of slope *vs* **7b** concentration to determine the K_i value for AChE inhibition. (C) LB plot for the inhibition of eqBChE by **7b**; (D) replot of slope *vs* **7b** concentration to determine the K_i value for BChE inhibition.

Further, it is found that it is the naphthyl moiety that enhances potency for BChE inhibition. The MD simulation studies revealed that **7b** does not induce conformational changes in both AChE and BChE. Further, **7b** also possesses high BBB permeability potential. Because of the dual ability of **7b** to inhibit both AChE and BChE enzymes, along with ability to inhibit Aβ-aggregation, and high BBB permeability potential, the further exploration of this scaffold is warranted in preclinical animal efficacy studies.

4. Experimental section

General. All chemicals were procured from TCI and Sigma-Aldrich Companies and were used as such without any further purification. The instruments used to record ^{1}H, ^{13}C, IR, and melting point data were same as described earlier [40]. The chemical shift values in ^{1}H and ^{13}C spectra were reported downfield to tetramethylsilane (TMS) in parts per million.

Generation of e-pharmacophore model and screening of a scaffold library. The human AChE protein (PDB: 4EY7) was retrieved and subjected for protein preparation under default set of conditions using Maestro v10.2 and Impact v6.7 (Schrodinger Inc., New York, 2015-2). Further, the complex was minimized by OPLS force field. Then, the grid file was constructed from the prepared protein by selecting co-crystallized ligand (donepezil) as centroid of cubic grid box. The donepezil was extracted from the prepared protein-ligand complex, minimized and redocked using XP Glide module under default setting. The PV file was used to develop the energy optimized pharmacophore. Pharmacophore features were

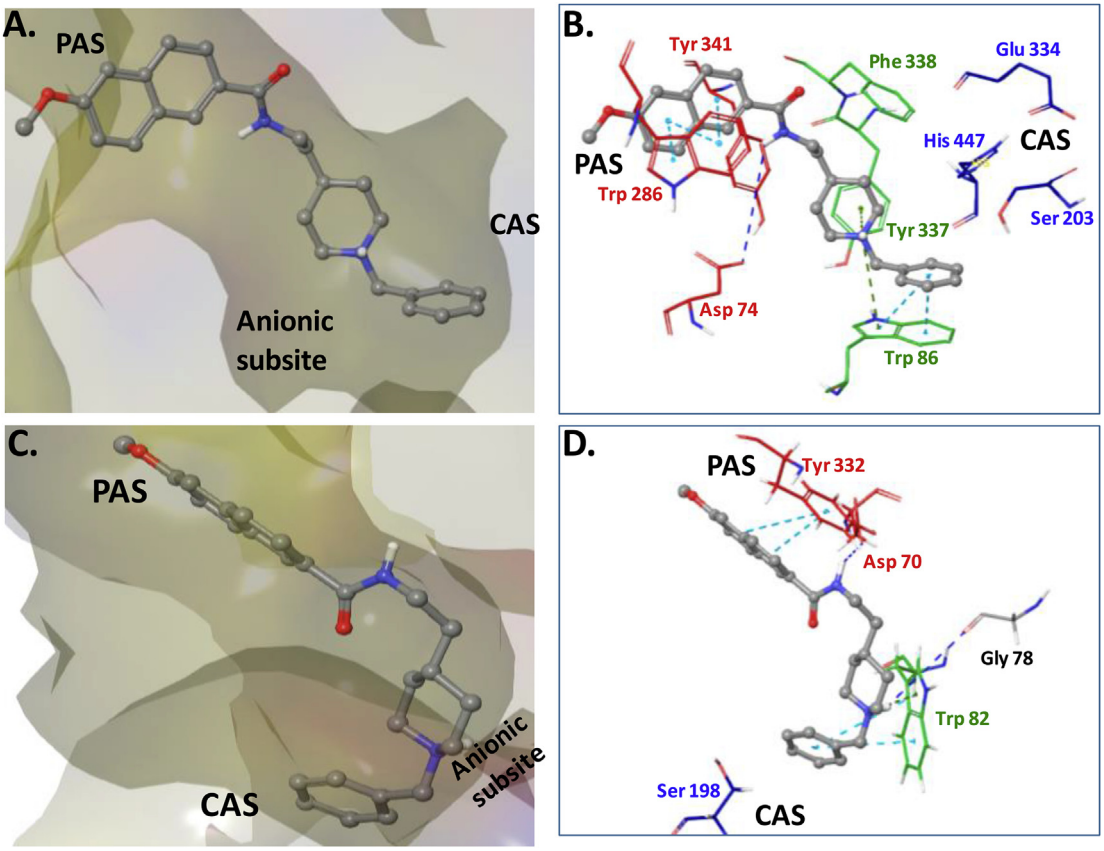

Fig. 5. Molecular docking of compound **7b** with human AChE (PDB ID: 4EY7) and human BChE (PDB ID: 6EP4). (A) Surface view of AChE showing the active site gorge and orientation of **7b** inside the gorge; (B) Interaction of **7b**with the active site of AChE. (C) Surface view of BChE showing the active site gorge and orientation of **7b** in the active site gorge; (F) Interaction of **7b** with the active site of BChE residues. The π-π interactions are represented by dark blue dotted lines; whereas the red dotted lines indicate H-bonding interactions. (For interpretation of the references to color in this figure legend, the reader is referred to the Web version of this article.)

generated using Phase module, which uses the default set of six chemical features containing hydrogen bond acceptor (A), hydrogen bond donor (D), hydrophobic (H), negative ionisable (N), positive ionisable (P) and aromatic ring (R). The advance pharmacophore screening panel of phase module was used to screen the compounds against the developed hypothesis under the default set of conditions. Out of the total six pharmacophore sites, ligands that match at least three features were ranked according to the fitness score.

General procedure for preparation of benzoyl chlorides 2a-w. To the solution of benzoic acids (2.4 mmol) in anhydrous THF (10 mL) under nitrogen atmosphere at 0 °C was slowly added oxalyl chloride (3.6 mmol). The reaction mixture was then stirred for 2–3 h under nitrogen. The reaction mixture was changed from transparent to a slightly yellowish color. The solvent was evaporated on vacuo rotavapor, and the obtained product was directly used for the next reaction.

General procedure for the preparation of amides 3a-w from benzoyl chlorides 2a-w. To the solution of benzoyl chlorides **2a-w** (1 equiv.) in anhydrous THF (10 mL) was added 4-aminopyridine (1 equiv.) under nitrogen atmosphere at 0 °C. The mixture was stirred for 5 min, and the reaction was monitored by TLC (R_f 0.5 in 10% MeOH: $CHCl_3$). After completion of the reaction, it was diluted with methanol. The resulting solution was concentrated on vacuo rotavapor to get the crude product, which was purified by silica gel (100–200) column chromatography using 5% MeOH: DCM as a mobile phase to get amides **3a-w** in 75–90% yield.

*3,5-Dimethoxy-N-(pyridin-4-yl)benzamide (**3a**)* [41]. Yield: 87%; white solid; m.p. 90–92 °C; ^{1}H NMR (400 MHz, $CDCl_3$) δ 8.63 (s, 1H), 8.38 (d, J = 5.2 Hz, 2H), 7.55 (d, J = 5.6 Hz, 2H), 7.39 (d, J = 4.5 Hz, 1H), 6.77 (d, J = 8.3 Hz, 1H), 3.82 (s, 3H), 3.80 (s, 3H). ESI-MS: *m/z* 259.0 $[M+H]^+$.

*3,5-Dimethoxy-N-(pyridin-4-yl)benzamide (**3b**)* [42]. Yield: 83%; white solid; m.p.201–203 °C; ^{1}H NMR (400 MHz, DMSO-d_6) δ 10.50 (s, 1H), 8.49 (d, J = 6.1 Hz, 2H), 7.78 (d, J = 6.2 Hz, 2H), 7.11 (d, J = 2.2 Hz, 2H), 6.76 (t, J = 2.1 Hz, 1H), 3.84 (s, 6H). ESI-MS: *m/z* 259.0 $[M+H]^+$.

*4-Chloro-N-(pyridin-4-yl)benzamide (**3c**)* [43]. Yield: 85%; white solid; m.p. 206–208 °C; ^{1}H NMR (400 MHz, DMSO-d_6) δ 10.65 (s, 1H), 8.50 (d, 2H), 8.00 (d, J = 8.5 Hz, 2H), 7.78 (d, J = 4.3 Hz, 2H), 7.65 (d, J = 8.5 Hz, 2H); ESI-MS: *m/z* 233.0 $[M+H]^+$.

*N-(Pyridin-4-yl)benzamide (**3d**)* [42,44]. Yield: 88%; white solid; m.p. 198–200 °C; ^{1}H NMR (400 MHz, DMSO-d_6) δ 10.59 (s, 1H), 8.49 (d, J = 5.8 Hz, 2H), 7.97 (d, J = 7.3 Hz, 2H), 7.80 (d, J = 6.1 Hz, 2H), 7.64 (t, J = 7.2 Hz, 1H), 7.57 (t, J = 7.5 Hz, 2H). ESI-MS: *m/z* 199.0 $[M+H]^+$.

*4-Isopropyl-N-(pyridin-4-yl)benzamide (**3e**).* Yield: 83%; white solid; m.p.109–111 °C; ^{1}H NMR (400 MHz, DMSO) δ 10.53 (s, 1H), 8.52 (d, J = 6.2 Hz, 2H), 7.95 (d, J = 8.3 Hz, 2H), 7.83 (dd, J = 4.9, 1.4 Hz, 2H), 7.47 (d, J = 8.3 Hz, 2H), 3.36 (s, 6H), 3.10–2.94 (m, 1H).ESI-MS: *m/z* 241.0 $[M+H]^+$.

*3-Chloro-N-(pyridin-4-yl)benzamide (**3f**)* [43]. Yield: 86%; white solid; m.p. 172–174 °C; ^{1}H NMR (400 MHz, DMSO-d_6) δ 10.72 (s, 1H), 8.55 (d, J = 5.9 Hz, 2H), 8.07 (s, 1H), 7.97 (d, J = 7.8 Hz, 1H), 7.82 (d, J = 6.3 Hz, 2H),7.54 (d, J = 8.0 Hz, 1H), 7.65 (t, J = 7.9 Hz, 1H). ESI-MS: *m/z* 233.0 $[M+H]^+$.

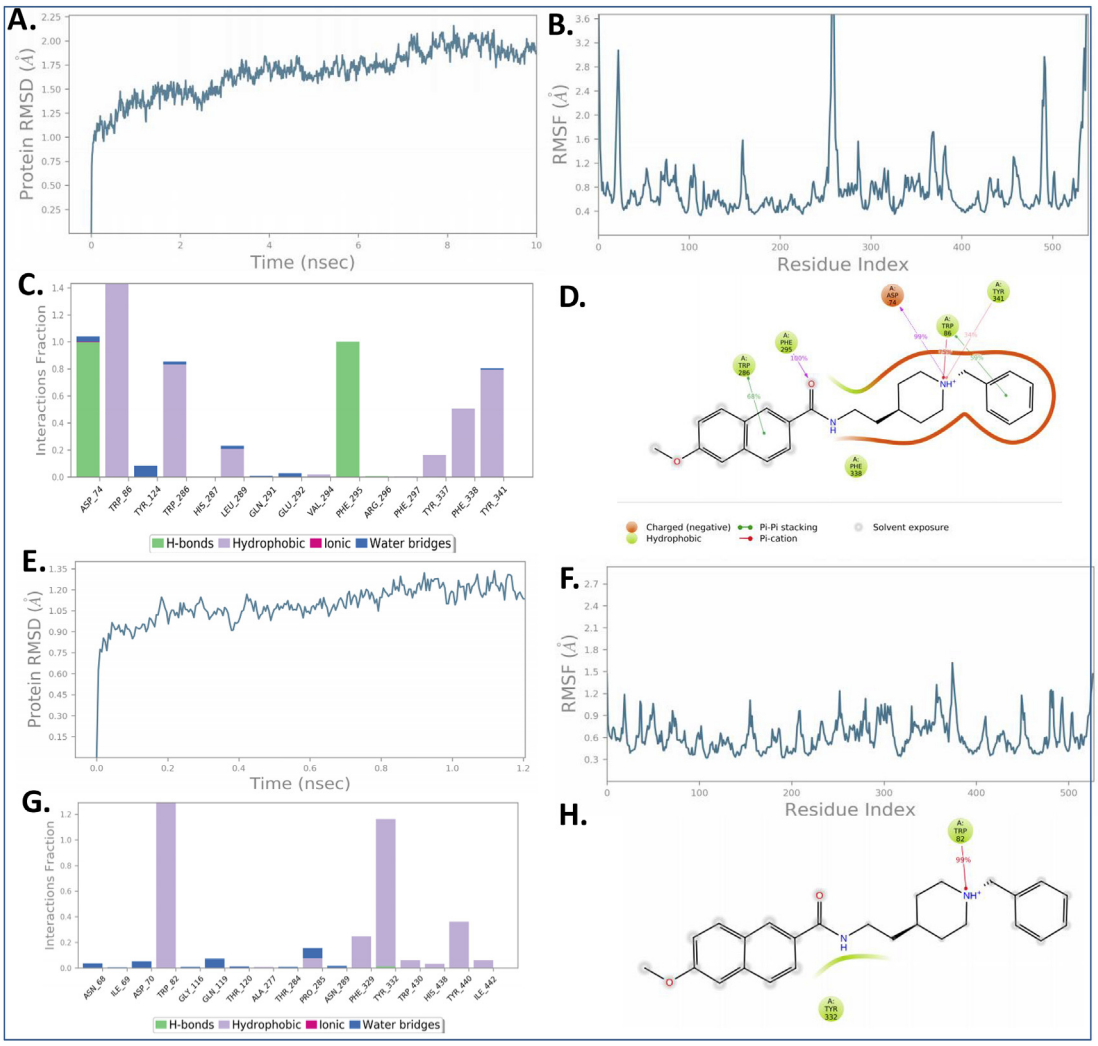

Fig. 6. MD simulation and interactions of compound **7b** with AChE and BChE. (A) RMSD in AChE enzyme C-α carbon during MD simulation; (B) RMSF in side chains of AChE during MD simulation. (C) Histogram showing interactions of **7b** with AChE; (D) 2D diagram for **7b** interactions with AChE; (E) RMSD in BChE enzyme C-α carbon during MD simulation; (F) RMSF in side chains of BChE during MD simulation; (G) Histogram showing interactions of **7b** with BChE; (H) 2D diagram for **7b** interactions with BChE.

6-Bromo-N-(pyridin-4-yl*)-2-naphthamide* (***3g***). Yield: 84%; white solid; m.p. 235–237 °C; ^{1}H NMR (400 MHz, DMSO-d_6) δ 10.80 (s, 1H), 8.62 (s, 1H), 8.52 (d, J = 6.1 Hz, 2H), 8.34 (s, 1H), 8.09 (d, J = 10.8 Hz, 3H), 7.83 (d, J = 6.2 Hz, 2H), 7.77 (dd, J = 8.8, 1.8 Hz, 1H). ESI-MS: *m/z* 327.0 $[M+H]^+$.

3-Bromo-N-(pyridin-4-yl*)benzamide* (***3i***). Yield: 75%; white solid; m.p.133–135 °C; ^{1}H NMR (400 MHz, $CDCl_3$) δ 8.56 (brs, 2H), 8.19 (s, 1H), 8.02 (brs, 1H), 7.80 (d, J = 7.7 Hz, 1H), 7.71 (d, J = 8.0 Hz, 1H), 7.62 (d, J = 5.3 Hz, 1H), 7.38 (t, J = 7.9 Hz, 1H). ESI-MS: *m/z* 276.0 $[M+H]^+$.

2-Methoxy-N-(pyridin-4-yl*)benzamide* (***3j***) [42]. Yield: 78%; white solid; m.p.178–179 °C; ^{1}H NMR (400 MHz, $CDCl_3$) δ 9.86 (s, 1H), 8.45 (d, J = 6.0 Hz, 2H), 8.19 (d, J = 9.3 Hz, 1H), 7.52 (d, J = 6.2 Hz, 2H), 7.46 (t, J = 7.8 Hz, 1H), 7.08 (t, J = 7.6 Hz, 1H), 6.98 (d, J = 8.3 Hz, 1H), 4.00 (s, 3H). ESI-MS: *m/z* 229.0 $[M+H]^+$.

4-Nitro-N-(pyridin-4-yl*)benzamide*(***3k***) [43].Yield: 77%; white solid; m.p. 248–250 °C; ^{1}H NMR (400 MHz, DMSO-d_6) δ 10.87 (s, 1H), 8.50 (s, 2H), 8.37 (d, J = 8.2 Hz, 2H), 8.17 (d, J = 8.3 Hz, 2H), 7.77 (s, 2H). ESI-MS: *m/z* 2244.0 $[M+H]^+$.

3,4-Dichloro-N-(pyridin-4-yl*)benzamide* (***3l***). Yield: 79%; white solid; m.p. 208–210 °C; ^{1}H NMR (400 MHz, DMSO-d_6) δ 10.78 (s, 1H), 8.57 (d, J = 4.0 Hz, 2H), 8.30 (s, 1H), 8.02 (d, J = 8.2 Hz, 1H), 7.91 (d, J = 8.3 Hz, 1H), 7.84 (d, J = 4.5 Hz, 2H).ESI-MS: *m/z* 267.0 $[M+H]^+$.

4*-Methoxy-N-(pyridin*-4-yl*)benzamide*(***3m***) [42].Yield: 81%; white solid; m.p.139–141 °C; ^{1}H NMR (400 MHz, $CDCl_3$) δ 8.43 (d, J = 4.7 Hz, 2H), 7.77 (d, J = 8.8 Hz, 2H), 7.52 (d, J = 5.3 Hz, 2H), 6.90 (d, J = 3.4 Hz, 2H), 3.79 (s, 3H). ESI-MS: *m/z* 229.0 $[M+H]^+$.

4-Cyano-N-(pyridin-4-yl*)benzamide* (***3n***) [44]. Yield: 89%; white solid; m.p. 203–205 °C; ^{1}H NMR (400 MHz, $CDCl_3$) δ 8.59 (d, J = 5.5 Hz, 2H), 7.98 (d, J = 8.2 Hz, 2H), 7.82 (d, J = 8.1 Hz, 2H), 7.60 (d, J = 5.9 Hz, 2H). ESI-MS: *m/z* 224.0 $[M+H]^+$.

3,4-Difluoro-N-(pyridin-4-yl*)benzamide* (***3o***).Yield: 88%; white solid; m.p. 174–176 °C; ^{1}H NMR (400 MHz, DMSO-d_6) δ 10.47 (s, 1H), 8.33 (d, J = 5.3 Hz, 2H), 7.91–7.86 (m, 1H), 7.71 (d, J = 7.2 Hz, 1H), 7.59 (d, J = 5.3 Hz, 2H), 7.52–7.45 (m, 1H). ESI-MS: *m/z* 235.0 $[M+H]^+$.

4-Ethoxy-N-(pyridin-4-yl*)benzamide* (***3p***).Yield: 90%; white solid; m.p.142–143 °C; ^{1}H NMR (400 MHz, DMSO) δ 10.44 (s, 1H), 8.50 (d, J = 5.3 Hz, 2H), 8.01 (d, J = 8.7 Hz, 2H), 7.83 (d, J = 5.9 Hz, 2H), 7.12 (d, J = 8.7 Hz, 2H), 4.21–4.12 (m, 2H), 1.41 (t, J = 7.0 Hz, 3H). ESI-MS:*m/z* 243.0 $[M+H]^+$.

3-Methoxy-N-(pyridin-4-yl*)benzamide* (***3q***). Yield: 87%; white solid; ^{1}H NMR (400 MHz, $CDCl_3$) δ 8.56 (d, J = 5.2 Hz, 2H), 7.98 (s,

1H), 7.61 (d, J = 5.4 Hz, 2H), 7.43–7.40 (m, 2H), 7.12 (d, J = 6.9 Hz, 1H), 3.88 (s, 3H). ESI-MS: *m/z* 229.0 $[M+H]^+$.

3-Chloro-4-fluoro-N-(pyridin-4-yl)benzamide (***3r***). Yield: 88%; white solid; m.p.168–170 °C; ^{1}H NMR (400 MHz, $CDCl_3$) δ 8.56 (d, J = 5.5 Hz, 2H), 8.07 (s, 1H), 7.97 (dd, J = 6.8, 2.1 Hz, 1H), 7.80–7.77 (m, 1H), 7.59 (d, J = 6.2 Hz, 2H). ESI-MS: *m/z* 251.0 $[M+H]^+$.

2,4-Dichloro-N-(pyridin-4-yl)benzamide (***3s***) [45]. Yield: 80%; white solid; m.p.172–174 °C; ^{1}H NMR (400 MHz, DMSO-d_6) δ 10.76 (s, 1H), 8.33 (d, J = 3.4 Hz, 2H), 7.63 (s, 1H), 7.52 (d, J = 2.8 Hz, 1H), 7.50 (d, J = 2.5 Hz, 2H), 7.42 (d, J = 8.2 Hz, 1H). ESI-MS: *m/z* 267.0 $[M+H]^+$.

4-Methyl-N-(pyridin-4-yl)benzamide (***3t***) [43]. Yield: 83%; white solid; m.p.161–163 °C; ^{1}H NMR (400 MHz, DMSO-d_6) δ 9.65 (s, 1H), 7.63 (d, J = 5.0 Hz, 2H), 7.05 (d, J = 7.1 Hz, 2H), 6.95 (d, J = 5.1 Hz, 2H), 6.53 (d, J = 7.8 Hz, 2H), 1.56 (s, 3H). ESI-MS: *m/z* 213.0 $[M+H]^+$.

N-(Pyridin-4-yl)furan-2-carboxamide (***3u***) [43]. Yield: 81%; white solid; m.p.158–160 °C; ^{1}H NMR (400 MHz, $CDCl_3$) δ 10.28 (s, 1H), 8.22 (d, J = 5.8 Hz, 2H), 7.74 (s, 1H), 7.52 (d, J = 6.2 Hz, 2H),7.17 (d, J = 3.5 Hz, 1H), 6.50 (dd, J = 3.4, 1.6 Hz, 1H). ESI-MS: *m/z* 189.0 $[M+H]^+$.

3,4,5-Trimethoxy-N-(pyridin-4-yl)benzamide (***3v***) [42,43]. Yield: 88%; white solid; m.p.165–167 °C; ^{1}H NMR (400 MHz, DMSO) δ 10.28 (s, 1H), 8.32 (d, J = 5.2 Hz, 2H), 7.59 (d, J = 5.3 Hz, 2H), 7.11 (s, 2H), 3.71 (s, 6H), 3.58 (s, 3H). ESI-MS: *m/z* 289.0 $[M+H]^+$.

General procedure for preparation of amides 3w-ac, 7a-b from carboxylic acids. To the solution of carboxylic acid (**1w-1ac**, 1 equiv.) in anhydrous DCM (10 mL) was added EDC.HCl (1.5 equiv.) and TEA (1equiv.) under nitrogen atmosphere at 0 °C. The mixture was stirred for 30 min, corresponding amines were added, and the mixture was again stirred for 1 h. The reaction was monitored by TLC (R_f: 0.5 in 10% MeOH: DCM). After completion of the reaction, the mixture was diluted with methanol. The resulting solution was concentrated on vacuo rotavapor to get the crude product, which was purified by silica gel (100–200) column chromatography using 5% MeOH: DCM as a mobile phase to get amides **3w-3ac, 7a-b** in 77–91% yield.

6-Methoxy-N-(pyridin-4-yl)-2-naphthamide (***3w***).Yield: 89%; white solid; m.p.187–189 °C; ^{1}H NMR (400 MHz, $CDCl_3$) δ 8.57 (d, J = 6.0 Hz, 2H), 8.32 (s, 1H), 8.08 (s, 1H), 7.90–7.83 (m, 3H), 7.65 (d, J = 6.2 Hz, 2H), 7.19 (d, J = 2.2 Hz, 1H), 3.96 (s, 3H). ESI-MS: *m/z* 279.0 $[M+H]^+$.

6-Methoxy-N-(pyridin-4-ylmethyl)-2-naphthamide (***3x***).Yield: 87%; white solid; m.p. 207–209 °C; ^{1}H NMR (400 MHz, $CDCl_3$) δ 8.58 (d, J = 5.9 Hz, 2H), 8.27 (s, 1H), 7.85–7.78 (m, 3H), 7.30 (d, J = 5.8 Hz, 2H), 7.21 (dd, J = 8.9, 2.4 Hz, 1H), 7.17 (d, J = 2.2 Hz, 1H), 4.72 (d, J = 6.0 Hz, 2H), 3.95 (s, 3H). ESI-MS: *m/z* 293.0 $[M+H]^+$.

6-Methoxy-N-(2-(pyridin-4-yl)ethyl)-2-naphthamide (***3y***). Yield: 89%; white solid; m.p.148–150 °C; ^{1}H NMR (400 MHz, $CDCl_3$) δ 8.54 (d, J = 5.5 Hz, 2H), 8.15 (s, 1H), 7.80–7.71 (m, 3H), 7.20–7.18 (m, 3H), 7.15 (d, J = 2.3 Hz, 1H), 3.94 (s, 3H), 3.79 (dd, J = 13.1, 6.8 Hz, 2H), 2.99 (t, J = 7.0 Hz, 2H).ESI-MS: *m/z* 307.0 $[M+H]^+$.

4-(Benzyloxy)-N-(pyridin-4-yl)benzamide (***3z***). Yield: 87%; white solid; m.p. 200–202 °C; IR (ν_{max}): 3358, 2906, 1692, 160500, 1605, 1511, 1422, 1345, 1276, 1167, 1122, 1020 cm^{-1};^{1}H NMR (400 MHz, CDCl3) δ 8.53 (d, J = 5.3 Hz, 2H), 7.84 (d, J = 8.5 Hz, 3H), 7.58 (d, J = 5.5 Hz, 2H), 7.44–7.34 (m, 4H), 7.06 (d, J = 8.5 Hz, 2H), 5.15 (s, 2H). ESI-MS: *m/z* 305.0 $[M+H]^+$.

4-Phenoxy-N-(pyridin-4-yl)benzamide (***3aa***).Yield: 85%; white solid; m.p. 157–159 °C; ^{1}H NMR (400 MHz, $CDCl_3$) δ 8.49 (d, J = 6.1 Hz, 2H), 7.85 (d, J = 8.7 Hz, 2H), 7.61 (d, J = 6.1 Hz, 2H), 7.39 (t, J = 7.9 Hz, 2H), 7.20 (t, J = 7.4 Hz, 1H), 7.07–7.01 (m, 4H). ESI-MS: *m/z* 291.0 $[M+H]^+$.

2-(4-(Benzyloxy)phenyl)-N-(pyridin-4-yl)acetamide (***3 ab***). Yield: 78%; white solid; m.p. 97–99 °C; ^{1}H NMR (400 MHz, $CDCl_3$) 8.44 (d, J = 4.7 Hz, 2H), 7.43 (t, J = 6.8 Hz, 3H), 7.39–7.33 (m, 4H), 7.22 (d, J = 8.3 Hz, 2H), 7.00 (dd, J = 8.5, 2.1 Hz, 2H), 5.08 (s, 2H), 3.69 (s, 2H). ESI-MS: *m/z* 319.0 $[M+H]^+$.

N-(Pyridin-4-yl)-[1,1′-biphenyl]-4-carboxamide (***3ac***). Yield: 77%; white solid; m.p. 250–252 °C; ^{1}H NMR (400 MHz, $CDCl_3$) δ 9.84 (s, 1H), 7.70 (d, J = 4.3 Hz, 2H), 7.29 (d, J = 8.1 Hz, 2H), 7.07 (d, J = 8.1 Hz, 2H), 7.03 (d, J = 4.9 Hz, 2H), 6.97 (d, J = 7.8 Hz, 2H), 6.72 (t, J = 7.5 Hz, 2H), 6.64 (t, J = 7.2 Hz, 1H). ESI-MS: *m/z* 275.0 $[M+H]^+$.

N-(1-Benzylpiperidin-4-yl)-6-methoxy-2-naphthamide (***7a***). Yield 91%; white solid; m.p. 186–187 °C; IR (ν_{max}): 3303, 3061, 2924, 2852, 2799, 2758, 2355, 1626, 1602, 1536, 1502, 1482, 1453, 1265, 1215, 1114, 1028 cm^{-1}; ^{1}H NMR (400 MHz, $CDCl_3$) δ 8.18 (s, 1H), 7.81 (d, J = 8.9 Hz, 1H), 7.77 (s, 2H), 7.33 (d, J = 4.6 Hz, 4H), 7.20 (d, J = 2.4 Hz, 1H), 7.18 (d, J = 2.4 Hz, 1H), 7.15 (d, J = 2.2 Hz, 1H), 3.94 (s, 3H), 3.56 (s, 2H), 2.90 (d, J = 11.8 Hz, 2H), 2.24 (t, J = 10.9 Hz, 2H), 2.07 (d, J = 10.5 Hz, 2H), 1.68 (s, 1H), 1.63 (d, J = 8.0 Hz, 2H); ^{13}C NMR (126 MHz, $CDCl_3$) δ 166.95, 159.04, 136.23, 130.42, 129.74, 129.24, 128.31, 128.03, 127.24, 127.12, 124.15, 119.74, 105.66, 63.00, 61.03, 55.38, 55.01, 52.32, 51.53, 47.01, 32.25; ESI-MS: *m/z* 375.0 $[M+H]^+$.

N-(2-(1-benzylpiperidin-4-yl)ethyl)-6-methoxy-2-naphthamide (***7b***).Yield: 89%; white solid; m.p. 140–142 °C; IR (ν_{max}): 3318, 3061, 3027, 2924, 2852, 2802, 2327, 1630, 1603, 1539, 1502, 1481, 1453, 1411, 1391, 1366, 1339, 1304, 1215, 1165, 1116 cm^{-1};^{1}H NMR (400 MHz, $CDCl_3$) δ 8.30 (s, 1H), 7.85 (d, J = 8.5 Hz, 1H), 7.79 (d, J = 8.9 Hz, 1H), 7.72 (d, J = 8.5 Hz, 1H), 7.46 (brs, 2H), 7.36 (brs, 3H), 7.16–7.12 (m, 2H), 6.98 (s, 1H), 3.95 (s, 2H), 3.91 (s, 3H), 3.49 (d, J = 6.2 Hz, 2H), 3.24 (d, J = 11.0 Hz, 2H), 2.48 (t, J = 10.7 Hz, 2H), 1.88–1.76 (m, 4H), 1.64–1.59 (m, 3H); ^{13}C NMR (126 MHz, $CDCl_3$) δ 167.64, 159.04, 136.22, 130.43, 129.72, 129.64, 128.42, 128.04, 127.65, 127.13, 124.16, 119.73, 105.65, 62.86, 55.39, 53.37, 37.76, 36.29, 33.22, 31.43. ESI-MS: *m/z* 403.0 $[M+H]^+$.

General procedure for preparation of *N*-benzylpyridinium salts 4a-au. To the solution of benzamides (**3a-3ac**), 0.5 mmol) in ACN (10 mL) was added halides (0.5 mmol) and resulting mixture was stirred at 80 °C for 1 h. The formation of white precipitate was observed in the reaction mixture. The precipitate was filtered and washed with acetone (10 mL × 3). The resulting residue was dried to get the desired *N*-benzylpyridinium salts **4a-4au** in 80–95% yield.

1-Benzyl-4-(3,4-dimethoxybenzamido)pyridin-1-ium bromide (***4a***).Yield: 90%; white solid; m.p.199–201 °C; IR (ν_{max}): 3584, 3396, 2913, 1684, 1600, 1604, 1513, 1461, 1324, 1265, 1173, 1134, 1019 cm^{-1}; ^{1}H NMR (400 MHz, DMSO-d_6) δ 11.48 (s, 1H), 8.98 (d, J = 6.8 Hz, 2H), 8.39 (d, J = 6.8 Hz, 2H), 7.75 (d, J = 8.4 Hz, 1H), 7.59 (s, 1H), 7.50 (d, J = 7.0 Hz, 2H), 7.46–7.41 (m, 3H), 7.15 (d, J = 8.5 Hz, 1H), 5.72 (s, 2H), 3.86 (s, 6H); ^{13}C NMR (126 MHz, CD_3OD): δ 166.98, 161.26, 153.79, 153.59, 149.19, 144.49, 133.81, 129.36, 129.24, 128.43, 124.89, 122.23, 115.78, 111.22, 110.66, 62.53, 55.29, 55.22. ESI-MS:*m/z* 349.0 $[M-Br]^+$.

1-Benzyl-4-(3,5-dimethoxybenzamido)pyridin-1-ium bromide (***4b***). Yield: 93%; white solid; m.p.232–235 °C; IR (ν_{max}): 3584, 3354, 2917, 2849, 2327, 1699, 1638, 1590, 1518, 1456, 1329, 1206, 1160, 1044 cm^{-1}; ^{1}H NMR (400 MHz, DMSO-d_6) δ 11.35 (s, 1H), 8.81 (d, J = 6.7 Hz, 2H), 8.17 (d, J = 6.6 Hz, 2H), 7.33–7.27 (m, 5H), 6.99 (d, J = 1.1 Hz, 2H), 6.67 (s, 1H), 5.55 (s, 2H), 3.68 (s, 6H); ^{13}C NMR (126 MHz, CD_3OD) δ 167.42, 161.26, 153.40, 144.61, 134.73, 133.75, 129.40, 129.26, 128.42, 115.96, 105.82, 104.63, 62.62, 54.80; ESI-MS:*m/z* 349.0 $[M-Br]^+$.

1-Benzyl-4-(4-chlorobenzamido)pyridin-1-ium bromide (***4c***). Yield: 93%; white solid; m.p.247–249 °C; IR (ν_{max}): 3073, 3029, 2923, 2850, 2337, 1695, 1639, 1596, 1455, 1327, 1256, 1205, 1162, 1096 cm^{-1}; ^{1}H NMR (400 MHz, DMSO-d_6) δ 11.46 (s, 1H), 8.78 (d, J = 6.7 Hz, 2H), 8.15 (d, J = 5.7 Hz, 2H), 7.86 (d, J = 8.3 Hz, 2H), 7.53 (d, J = 8.5 Hz, 2H), 7.29–7.24 (m, 5H), 5.54 (s, 2H); ^{13}C NMR (101 MHz, CD_3OD) δ 166.69, 153.38, 144.70, 139.31, 133.71, 131.56, 129.66, 129.42, 129.28, 128.78, 128.43, 115.99, 62.70. ESI-MS:*m/z* 323.0 $[M-Br]^+$.

*4-Benzamido-1-benzylpyridin-1-ium bromide (**4d**).*Yield: 91%; white solid; m.p.272–275 °C; IR (ν_{max}): 3378, 3127, 3067, 2951, 2852, 1694, 1518, 1258, 1206, 1164 cm^{-1}; ^1H NMR (400 MHz, MeOD) δ 8.86 (d, $J = 7.3$ Hz, 2H), 8.42 (d, $J = 7.3$ Hz, 2H), 8.07–8.04 (m, 2H), 7.71 (t, $J = 7.4$ Hz, 1H), 7.60 (t, $J = 7.6$ Hz, 2H), 7.52–7.49 (m, 3H), 5.72 (s, 1H); ^{13}C NMR (126 MHz, CD_3OD) δ 167.76, 153.46, 144.65, 133.77, 133.05, 132.92, 129.39, 129.25, 128.55, 128.45, 127.94, 115.91, 62.62. ESI-MS:*m/z* 289.0 $[M - Br]^+$.

*1-Benzyl-4-(4-isopropylbenzamido)pyridin-1-ium bromide (**4e**).* Yield: 90%; white solid; m.p. 247–250 °C; IR (ν_{max}): 3390, 3188, 3029, 2966, 2782, 2327, 1691, 1641, 1608, 1591, 1519, 1461, 1327, 1259, 1161 cm^{-1}; ^1H NMR (400 MHz, CD_3OD) δ 8.82 (d, $J = 7.5$ Hz, 2H), 8.40 (d, $J = 7.4$ Hz, 2H), 7.99 (d, $J = 8.4$ Hz, 2H), 7.52–7.46 (m, 4H), 5.70 (s, 2H), 3.05 (m, 1H), 1.33 (d, $J = 6.9$ Hz, 6H). ^{13}C NMR (126 MHz, CD_3OD) δ 167.59, 154.97, 153.52, 144.59, 133.80, 130.39, 129.37, 129.25, 128.45, 128.23, 126.62, 115.84, 62.57, 34.11, 22.65. ESI-MS:*m/z* 331.0 $[M - Br]^+$.

*1-Benzyl-4-(3-chlorobenzamido)pyridin-1-ium bromide (**4f**).*Yield: 92%; white solid; m.p.274–277 °C; IR (ν_{max}): 3584, 3330, 2922, 2851, 2342, 1740, 1695, 1638, 1517, 1453, 1323, 1248, 1207, 1160 cm^{-1}; ^1H NMR (400 MHz, DMSO-d_6) δ 11.66 (s, 1H), 8.98 (d, $J = 6.6$ Hz, 2H), 8.32 (d, $J = 6.8$ Hz, 2H), 8.08 (s, 1H), 7.97 (d, $J = 8.2$ Hz, 1H), 7.80 (d, $J = 8.0$ Hz, 1H), 7.66 (t, $J = 7.9$ Hz, 1H), 7.48–7.45 (m, 5H), 5.75 (s, 2H); ^{13}C NMR (126 MHz, CD_3OD) δ 164.82, 151.75, 143.20, 133.33, 133.05, 132.20, 131.32, 128.67, 127.89, 127.74, 126.90, 126.40, 124.82, 114.51, 61.16. ESI-MS:*m/z* 323.0 $[M - Br]^+$.

*1-Benzyl-4-(6-bromo-2-naphthamido)pyridin-1-ium bromide (**4g**).* Yield: 91%; white solid; m.p. 336–338 °C; IR (ν_{max}): 3584, 3238, 2923, 2852, 2342, 1741, 1687, 1627, 1588, 1517, 1454, 1322, 1287, 1230 cm^{-1}; ^1H NMR (400 MHz, DMSO-d_6) δ 11.82 (s, 1H), 8.99 (d, $J = 6.8$ Hz, 2H), 8.72 (s, 1H), 8.39–8.37 (m, 3H), 8.14–8.08 (m, 3H), 7.81 (d, $J = 8.8$ Hz, 1H), 7.51–7.46 (m, 5H), 5.74 (s, 2H); ^{13}C NMR (126 MHz, DMSO-d_6): δ 167.58, 153.15, 146.98, 145.72, 140.65, 136.42, 135.13, 131.85, 130.88, 130.33, 129.97, 129.70, 129.00, 128.84, 128.25, 125.99, 122.71, 116.59, 62.26. ESI-MS:*m/z* 418.0 $[M - Br]^+$.

*1-Benzyl-4-(2-bromo-4-flourobenzamido)pyridin-1-ium bromide (**4h**).*Yield: 89%; white solid; m.p.225–228 °C; IR (ν_{max}): 3069, 2922, 2852, 2343, 2046, 1704, 2638, 1597, 1518, 1462, 1326, 1204 cm^{-1}; ^1H NMR (400 MHz, DMSO-d_6) δ 11.95 (s, 1H), 9.00 (d, $J = 6.7$ Hz, 2H), 8.23 (d, $J = 6.7$ Hz, 2H), 7.99 (d, $J = 5.9$ Hz, 1H), 7.90–7.88 (m, 1H), 7.50–7.42 (m, 6H), 5.75 (s, 2H); ^{13}C NMR (126 MHz, CD_3OD) δ 163.36, 160.02, 158.01, 152.58, 145.00, 137.00, 136.93, 133.65, 132.78, 129.43, 129.27, 128.51, 124.28, 124.16, 118.50, 118.31, 116.74, 116.71, 115.97, 62.79. ESI-MS:*m/z* 385.0 $[M - Br]^+$.

*1-Benzyl-4-(3-bromobenzamido)pyridin-1-ium bromide (**4i**).*Yield: 93%; white solid; m.p. 247–250 °C; IR (ν_{max}): 3069, 3014, 2925, 2852, 1694, 1638, 1597, 1518, 1455, 1280, 1248, 1205, 1162 cm^{-1}; ^1H NMR (400 MHz, DMSO-d_6) δ 11.66 (s, 1H), 8.98 (d, $J = 5.7$ Hz, 2H), 8.33 (d, $J = 6.9$ Hz, 2H), 8.21 (s, 1H), 8.01 (d, $J = 7.8$ Hz, 1H), 7.92 (d, $J = 8.0$ Hz, 1H), 7.59 (t, $J = 7.9$ Hz, 1H), 7.48–7.45 (m, 5H), 5.73 (s, 2H); ^{13}C NMR (126 MHz, CD_3OD) δ 166.24, 153.25, 144.72, 135.83, 135.02, 133.72, 130.86, 130.38, 129.41, 129.26, 128.44, 126.78, 122.34, 116.05, 62.69. ESI-MS:*m/z* 368.0 $[M - Br]^+$.

*1-Benzyl-4-(2-methoxybenzamido)pyridin-1-ium bromide (**4j**).*Yield: 94%; white solid; m.p. 192–194 °C; IR (ν_{max}): 3295, 3163, 3125, 3027, 2917, 2849, 1694, 1639, 1591, 1519, 1464, 1328, 1162 cm^{-1}; ^1H NMR (400 MHz, DMSO-d_6) δ 11.51 (s, 1H), 8.94 (d, $J = 7.0$ Hz, 2H), 8.25 (d, $J = 6.8$ Hz, 2H), 7.61 (t, $J = 8.1$ Hz, 2H), 7.49–7.39 (m, 5H), 7.25 (d, $J = 8.1$ Hz, 1H), 7.12 (t, $J = 7.4$ Hz, 1H), 5.71 (s, 2H), 3.89 (s, 3H); ^{13}C NMR (126 MHz, CD_3OD) δ 166.39, 157.74, 152.61, 144.69, 134.44, 133.75, 130.99, 129.38, 129.35, 128.42, 121.37, 120.89, 115.87, 111.85, 62.61, 55.48. ESI-MS:*m/z* 319.0 $[M - Br]^+$.

1-Benzyl-4-(4-nitrobenzamido)pyridin-1-ium bromide (**4k**) [46]. Yield: 95%; yellow solid; m.p. 205–208 °C; IR (ν_{max}): 3584, 3384, 3018, 2954, 2917, 2894, 2327, 1693, 1604, 1517, 1456, 1251, 1172 cm^{-1}; ^1H NMR (400 MHz, DMSO-d_6) δ 11.85 (s, 1H), 9.04 (d, $J = 6.8$ Hz, 2H), 8.37 (d, $J = 6.7$ Hz, 2H), 8.19 (d, $J = 8.1$ Hz, 2H), 8.11 (d, $J = 8.2$ Hz, 2H), 7.52–7.43 (m, 5H); ^{13}C NMR (126 MHz, CD_3OD) δ 166.12, 153.08, 150.51, 144.86, 138.44, 133.66, 129.44, 129.39, 129.27, 128.47, 123.47, 116.20, 62.80. ESI-MS:*m/z* 334.0 $[M - Br]^+$.

*1-Benzyl-4-(3,4-dichlorobenzamido)pyridin-1-ium bromide (**4l**).*Yield: 91%; white solid; m.p. 299–301 °C; IR (ν_{max}): 3583, 3396, 2917, 2849, 2351, 1692, 1518, 1455, 1326, 1164 cm^{-1}; ^1H NMR (400 MHz, DMSO-d_6) δ 11.56 (s, 1H), 8.85 (d, $J = 6.7$ Hz, 2H), 8.17 (d, $J = 6.8$ Hz, 2H), 8.12 (s, 1H), 7.83 (d, $J = 8.4$ Hz, 1H), 7.72 (d, $J = 8.4$ Hz, 1H), 7.33–7.26 (m, 5H), 5.58 (s, 2H); ^{13}C NMR (126 MHz, CD_3OD) δ 163.99, 152.28, 143.27, 135.91, 132.19, 131.61, 131.25, 129.32, 129.20, 128.53, 127.95, 127.78, 126.94, 126.19, 114.61. ESI-MS:*m/z* 357.0 $[M - Br]^+$.

1-Benzyl-4-(4-methoxybenzamido)pyridin-1-ium bromide (**4m**) [46]. Yield: 92%; white solid; m.p. 261–265 °C; IR (ν_{max}): 3584, 3013, 2917, 1692, 1639, 1604, 1517, 1456, 1321, 1251, 1173 cm^{-1}; ^1H NMR (400 MHz, DMSO-d_6) δ 11.48 (s, 1H), 8.98 (d, $J = 6.8$ Hz, 2H), 8.37 (d, $J = 6.6$ Hz, 2H), 8.06 (d, $J = 8.4$ Hz, 2H), 7.51–7.42 (m, 5H), 7.41 (d, $J = 8.8$ Hz, 2H), 5.73 (s, 2H), 3.87 (s, 3H); ^{13}C NMR (126 MHz, CD_3OD) δ 165.51, 162.56, 152.15, 143.00, 132.32, 128.72, 127.87, 127.75, 126.92, 123.25, 114.23, 112.30, 61.03, 53.30. ESI-MS:*m/z* 319.0 $[M - Br]^+$.

*1-Benzyl-4-(4-cyanobenzamido)pyridin-1-ium bromide (**4n**).* Yield: 95%; white solid; m.p. 235–237 °C; IR (ν_{max}): 3396, 3072, 2918, 2849, 2231, 1698, 1639, 1594, 1518, 1326, 1257, 1206, 1163 cm^{-1}; ^1H NMR (400 MHz, CD_3OD) δ 11.85 (s, 1H), 8.89 (d, $J = 7.4$ Hz, 2H), 8.42 (d, $J = 7.4$ Hz, 2H), 8.11 (d, $J = 8.2$ Hz, 2H), 7.98 (d, 2H), 7.52–7.43 (m, 5H), 5.74 (s, 2H);^{13}C NMR (126 MHz, CD_3OD) δ 166.32, 153.09, 144.84, 136.93, 133.74, 132.39, 129.43, 129.27, 128.78, 128.50, 117.38, 116.14, 62.72. ESI-MS:*m/z* 314.2$[M - Br]^+$.

*1-Benzyl-4-(3,4-difluorobenzamido)pyridin-1-ium bromide (**4o**).* Yield: 89%; white solid; m.p.215–217 °C; IR (ν_{max}): 1584, 3074, 3029, 2952, 2852, 2062, 1699, 1640, 1594, 1515, 1456, 1326, 1277 cm^{-1}; ^1H NMR (400 MHz, DMSO-d_6) δ 8.88 (d, $J = 6.9$ Hz, 2H), 8.21 (d, $J = 6.9$ Hz, 2H), 8.02–7.97 (m, 1H), 7.79 (d, $J = 6.6$ Hz, 1H), 7.52 (dd, $J = 18.5$, 8.6 Hz, 1H), 7.34 (d, $J = 7.2$ Hz, 2H), 7.28–7.23 (m, 3H), 5.60 (s, 2H); ^{13}C NMR (126 MHz, CD_3OD) δ 165.40, 154.45, 154.36, 153.22, 152.33, 151.15, 144.74, 133.71, 130.21, 129.41, 129.26, 128.46, 125.51, 117.70, 117.55, 116.05, 62.70. ESI-MS:*m/z* 325.1 $[M - Br]^+$.

*1-Benzyl-4-(4-ethoxybenzamido)pyridin-1-ium bromide (**4p**).*Yield: 90%; white solid; m.p. 261–263 °C; IR (ν_{max}): 2926, 2848, 2328, 1690, 1639, 1605, 1518, 1455, 1319, 1248, 1173 cm^{-1}; ^1H NMR (400 MHz, DMSO-d_6) δ 11.43 (s, 1H), 8.94 (d, $J = 4.8$ Hz, 2H), 8.33 (d, $J = 5.4$ Hz, 2H), 8.03 (d, $J = 8.2$ Hz, 2H), 7.48–7.41 (m, 5H), 7.13 (d, $J = 8.7$ Hz, 2H), 5.70 (s, 2H), 4.16 (q, $J = 6.9$ Hz, 2H), 1.37 (t, $J = 6.9$ Hz, 3H); ^{13}C NMR (126 MHz, CD_3OD) δ 167.02, 163.38, 153.67, 144.48, 133.81, 130.19, 129.37, 129.25, 128.38, 124.55, 115.69, 114.21, 63.68, 62.51, 13.56. ESI-MS:*m/z* 333.0 $[M - Br]^+$.

*1-Benzyl-4-(3-methoxybenzamido)pyridin-1-ium bromide (**4q**).* Yield: 93%; white solid; m.p. 170–172 °C; IR (ν_{max}): 2926, 2848, 2328, 1690, 1639, 1605, 1518, 1455, 1319, 1248, 1173 cm^{-1}; ^1H NMR (400 MHz, DMSO) δ 11.56 (s, 1H), 8.96 (d, $J = 6.0$ Hz, 2H), 8.34 (d, $J = 6.2$ Hz, 2H), 7.60 (d, $J = 7.6$ Hz, 1H), 7.54 (t, $J = 7.7$ Hz, 2H), 7.48–7.43 (m, 5H), 7.29 (d, $J = 8.1$ Hz, 1H), 5.72 (s, 2H), 3.86 (s, 3H); ^{13}C NMR (126 MHz, CD_3OD) δ 167.53, 160.07, 153.40, 144.63, 134.17, 133.76, 129.68, 129.38, 129.25, 128.47, 120.03, 118.84, 115.96, 113.15, 62.62, 54.72. ESI-MS:*m/z*319.0 $[M - Br]^+$.

*1-Benzyl-4-(3-chloro-4-fluorobenzamido)pyridin-1-ium bromide (**4r**).* Yield: 88%; white solid; m.p. 245–247 °C; IR (ν_{max}): 3387, 3026, 2923, 2851, 2347, 1695, 1640, 1600, 1517, 1456, 1325, 1207 cm^{-1}; ^1H NMR (400 MHz, DMSO-d_6) δ 11.47 (s, 1H), 8.79 (d,

J = 5.4 Hz, 2H), 8.13 (d, J = 6.3 Hz, 2H), 7.87 (s, 1H), 7.51 (t, J = 8.9 Hz, 1H), 7.29–7.26 (m, 5H), 5.54 (s, 2H); ^{13}C NMR (126 MHz, CD_3OD) δ 165.38, 162.14, 159.89, 153.24, 144.74, 144.74, 133.72, 133.72, 130.91, 130.91, 129.42, 129.26, 129.14, 129.14, 129.07, 129.07, 128.43, 116.97, 116.79, 116.04, 62.70. ESI-MS: m/z 341.0 $[M - Br]^+$.

*1-Benzyl-4-(2,4-dichlorobenzamido)pyridin-1-ium bromide (**4s**).* Yield: 90%; white solid; m.p. 247–249 °C; IR (ν_{max}): 3383, 2921, 2848, 1706, 1639, 1593, 1518, 1455, 1326, 1273 cm^{-1}; ^{1}H NMR (400 MHz, DMSO-d_6) δ 12.06 (s, 1H), 9.02 (d, J = 6.9 Hz, 2H), 8.23 (d, J = 6.9 Hz, 2H), 7.86 (s, 1H), 7.77 (d, J = 8.3 Hz, 1H), 7.66 (dd, J = 8.3, 1.3 Hz, 1H), 7.51–7.43 (m, 5H), 5.77 (s, 2H); ^{13}C NMR (126 MHz, CD_3OD) δ 166.29, 152.55, 145.08, 137.46, 133.65, 133.22, 131.99, 130.21, 129.79, 129.43, 129.27, 128.49, 127.45, 115.79, 62.80. ESI-MS:m/z 357.0 $[M - Br]^+$.

*1-Benzyl-4-(4-methylbenzamido)pyridin-1-ium bromide (**4t**)* [47]. Yield: 91%; white solid; m.p. 276–278 °C; IR (ν_{max}): 3123, 3068, 3030, 2952, 2918, 2849, 2355, 1693, 1639, 1591, 1518, 1455, 1327, 1259, 1205, 1163, 1084 cm^{-1}; ^{1}H NMR (400 MHz, DMSO-d_6) δ 11.52 (s, 1H), 8.95 (d, J = 6.4 Hz, 2H), 8.34 (d, J = 7.0 Hz, 2H), 7.95 (d, J = 7.9 Hz, 2H), 7.48–7.42 (m, 7H), 5.71 (s, 3H), 2.43 (s, 2H); ^{13}C NMR (126 MHz, DMSO-d_6) δ 167.47, 153.22, 145.59, 144.25, 135.19, 130.42, 129.77, 129.68, 129.63, 128.99, 128.95, 116.46, 62.13, 21.63. ESI-MS: m/z 303.0 $[M - Br]^+$.

*1-Benzyl-4-(furan-2-carboxamido)pyridin-1-ium bromide (**4u**).* Yield: 93%; white solid; m.p. 239–241 °C; IR (ν_{max}): 3583, 3387, 2918, 2849, 2343, 1691, 1641, 1596, 1518, 1467, 1327, 1273, 1218, 1173 cm^{-1}; ^{1}H NMR (400 MHz, DMSO-d_6) δ 11.61 (s, 1H), 8.97 (d, J = 6.4 Hz, 2H), 8.35 (d, J = 6.6 Hz, 2H), 8.11 (s, 1H), 7.66 (s, 1H), 7.49–7.44 (m, 5H), 6.82–6.81 (m, 1H), 5.72 (s, 2H); ^{13}C NMR (126 MHz, CD_3OD) δ 157.37, 153.06, 147.12, 146.17, 144.63, 133.73, 129.39, 129.25, 128.43, 118.05, 115.83, 112.63, 62.62; ESI-MS:m/z279.2$[M - Br]^+$.

*1-Benzyl-4-(3,4,5-trimethoxybenzamido)pyridin-1-ium bromide (**4v**).* Yield 91%; white solid, m.p. 180–181 °C; IR 3418, 2954, 2924, 2350, 1691, 1639, 1586, 1518, 1503, 1461, 1416, 1202, 1171, 1125 cm^{-1}; ^{1}H NMR (400 MHz, DMSO-d_6) δ 11.48 (s, 1H), 8.97 (d, J = 7.2 Hz, 2H), 8.33 (d, J = 6.1 Hz, 2H), 7.48–7.43 (m, 5H), 7.33 (d, J = 2.9 Hz, 2H), 5.71 (s, 2H), 3.89 (s, 6H), 3.77 (s, 3H); ^{13}C NMR (101 MHz, DMSO-d_6) δ 167.10, 153.20, 153.11, 145.51, 142.08, 135.09, 129.70, 129.67, 128.99, 128.22, 116.53, 106.62, 62.17, 60.72, 56.74; ESI-MS:m/z 379.0 $[M - Br]^+$.

*1-Benzyl-4-(6-methoxy-2-naphthamido)pyridin-1-ium bromide (**4w**).* Yield: 87%; white solid; m.p. 296–298 °C; IR (ν_{max}): 3286, 2954, 2922, 2885, 2870, 2367, 2351, 2344, 2312, 1624, 1583, 1517, 1454, 1377, 1317, 1286, 1265, 1197, 1158, 1024 cm^{-1}; ^{1}H NMR (400 MHz, MeOD) δ 8.82 (d, J = 7.1 Hz, 2H), 8.58 (s, 1H), 8.43 (d, J = 7.0 Hz, 2H), 8.02 (d, J = 8.6 Hz, 1H), 7.96 (t, J = 8.8 Hz, 2H), 7.50 (s, 5H), 7.38 (d, J = 1.7 Hz, 1H), 7.29 (dd, J = 9.0, 2.1 Hz, 1H), 5.69 (s, 2H), 3.98 (s, 3H); ^{13}C NMR (101 MHz, DMSO-d_6) δ 167.72, 159.93, 153.25, 145.51, 137.30, 135.05, 131.40, 129.88, 129.72, 129.69, 128.99, 128.05, 127.76, 127.60, 125.33, 120.43, 116.45, 106.56, 62.22, 55.96. ESI-MS: m/z 369.0 $[M - Br]^+$.

*4-(6-Methoxy-2-naphthamido)-1-(2-methylbenzyl)pyridin-1-ium bromide (**4x**).*Yield: 90%; white solid; m.p. 189–191 °C; IR (ν_{max}): 3500, 2920, 2343, 2148, 1684,1623, 1590, 1515, 1479, 1454, 1434, 1395, 1323, 1288, 1265, 1066, 1041 cm^{-1}; ^{1}H NMR (400 MHz, DMSO-d_6) δ 8.65 (d, J = 6.6 Hz, 2H), 8.53 (s, 1H), 8.29 (d, J = 5.0 Hz, 2H), 8.01–7.95 (m, 3H), 7.45–7.24 (m, 5H), 7.18 (d, J = 7.4 Hz, 1H), 5.65 (s, 2H), 2.25 (s, 3H); ^{13}C NMR (126 MHz, DMSO-d_6) δ 167.71, 159.94, 153.32, 145.72, 137.33, 133.13, 131.39, 129.99, 129.70, 129.48, 127.71, 127.63, 127.16, 125.40, 120.42, 116.41, 106.61, 60.40, 55.98, 19.26.ESI-MS:m/z 383.0 $[M - Br]^+$.

*1-(4-Methoxy)-4-(6-methoxy-2-naphthamido)pyridin-1-ium chloride (**4y**).*Yield: 91%, white solid; m.p. 259–261 °C; IR (ν_{max}): 2955, 2923, 2852, 2350, 2327, 1830, 1792, 1729, 1700, 1691, 1663, 1653, 1635, 1624, 1570, 1559, 1540, 1483, 1331, 1278, 1200, 1190, 1158, 1081, 1028 cm^{-1}; ^{1}H NMR (400 MHz, MeOD) δ 12.71 (s, 1H), 9.75 (d, J = 6.9 Hz, 2H), 9.54 (s, 1H), 9.25 (d, J = 6.9 Hz, 2H), 8.87–8.77 (m, 3H), 8.0–8.26 (m, 3H), 8.11 (d, J = 8.9 Hz, 1H), 7.81 (d, J = 8.4 Hz, 2H), 6.43 (s, 2H), 4.73 (s, 3H), 4.57 (s, 3H); ^{13}C NMR (101 MHz, DMSO) δ 169.11, 161.81, 161.38, 154.72, 146.62, 138.72, 132.83, 132.28, 131.47, 129.42, 129.07, 128.34, 126.84, 121.73, 117.87, 116.48, 108.05, 63.27, 57.38, 57.17. ESI-MS:m/z 399.0$[M - Cl]^+$.

*1-(2-Chlorobenzyl)-4-(6-Methoxy-2-naphthamido)pyridin-1-ium chloride (**4z**).*Yield: 90%; white solid; m.p. 255–257 °C; IR (ν_{max}): 3420, 2355, 2348, 1734, 1684, 1653, 1593, 1517,1481, 1457, 1324, 1269, 1201, 1164, 1073 cm^{-1}; ^{1}H NMR (400 MHz, DMSO-d_6) δ 12.11 (s, 1H), 8.78 (d, J = 6.6 Hz, 2H), 8.75 (s, 1H), 8.46 (d, J = 6.5 Hz, 2H), 7.98 (d, J = 8.6 Hz, 1H), 7.90–7.83 (m, 2H), 7.47 (d, J = 7.3 Hz, 1H), 7.38–7.32 (m, 4H), 7.16 (d, J = 8.9 Hz, 1H), 5.72 (s, 2H), 3.80 (s, 3H); ^{13}C NMR (126 MHz, DMSO-d_6) δ 167.76, 159.93, 153.77, 145.84, 137.32, 133.58, 132.45, 131.70, 131.46, 130.54, 130.41, 128.61, 127.85, 127.63, 127.57, 125.58, 120.30, 116.36, 106.54, 60.01, 55.95.ESI-MS: m/z403.0 $[M - Cl]^+$.

*1-(3-Chlorobenzyl)-4-(6-methoxy-2-naphthamido)pyridin-1-ium chloride (**4aa**).* Yield: 91%, white solid; m.p. 260–262 °C; IR (ν_{max}): 2920, 2352, 2344, 1734, 1700, 1683, 1653, 1640, 1623, 1554, 1558, 1521, 1476, 1456, 1395, 1317, 1278, 1263, 1195, 1163, 1068, 1032 cm^{-1}; ^{1}H NMR (400 MHz, DMSO) δ 12.27 (s, 1H), 9.11 (d, J = 6.9 Hz, 2H), 8.94 (s, 1H), 8.64 (d, J = 6.9 Hz, 2H), 8.18 (d, J = 8.5 Hz, 1H), 8.09–8.02 (m, 2H), 7.75 (s, 1H), 7.56 (s, 3H), 7.52 (s, 1H), 7.36 (dd, J = 8.8, 1.7 Hz, 1H), 5.82 (s, 2H), 4.00 (s, 3H); ^{13}C NMR (126 MHz, DMSO-d_6) δ 167.72, 159.93, 153.64, 145.55, 137.48, 137.31, 134.13, 131.55, 131.44, 130.35, 129.59, 129.08, 127.87, 127.81, 127.63, 127.58, 125.55, 120.29, 116.52, 106.56, 61.16, 55.95.ESI-MS: m/z403.0 $[M - Cl]^+$.

*1-(4-Chlorobenzyl)-4-(6-methoxy-2-naphthamido)pyridin-1-ium chloride (**4 ab**).*Yield: 91%; white solid; m.p. 256–258 °C; IR (ν_{max}): 2918, 2355, 2340, 1729, 1691, 1641, 1623, 1554, 1517, 1482, 1453, 1333, 1279, 1215, 1190, 1160, 1026 cm^{-1}; ^{1}H NMR (400 MHz, DMSO-d_6) δ 12.04 (s, 1H), 8.98 (d, J = 7.0 Hz, 2H), 8.79 (s, 1H), 8.51 (d, J = 7.0 Hz, 2H), 8.08–7.97 (m, 3H), 7.58–7.50 (m, 4H), 7.46 (s, 1H), 7.30 (d, J = 8.6 Hz, 1H), 5.73 (s, 2H), 3.93 (s, 3H); ^{13}C NMR (101 MHz, DMSO-d_6) δ 167.74, 159.98, 153.66, 145.51, 137.34, 134.96, 134.45, 134.19, 131.47, 131.11, 130.42, 129.66, 127.88, 127.68, 127.59, 125.59, 120.29, 116.54, 106.62, 61.18, 55.99.ESI-MS:m/z 403.0 $[M - Cl]^+$.

*1-(2-Fluorobenzyl)-4-(6-methoxy-2-naphthamido)pyridin-1-ium bromide (**4ac**).* Yield: 93%; white solid; m.p. 276–277 °C; IR (ν_{max}): 3386, 2377, 2343, 1824, 1767, 1729, 1712, 1690, 1680, 1659, 1642, 1538, 1516, 1502, 1486, 1469, 1415, 1322, 1262, 1194, 1023 cm^{-1}; ^{1}H NMR (400 MHz, MeOD) δ 8.81 (d, J = 7.2 Hz, 2H), 8.57 (s, 1H), 8.43 (d, J = 7.2 Hz, 2H), 8.02 (d, J = 8.6 Hz, 1H), 7.96 (t, J = 8.3 Hz, 2H), 7.61 (t, J = 7.4 Hz, 1H), 7.58–7.53 (m, 1H), 7.38 (d, J = 2.2 Hz, 1H), 7.34 (d, J = 7.3 Hz, 1H), 7.29 (dd, J = 9.1, 2.0 Hz, 2H), 5.77 (s, 2H), 3.99 (s, 3H); ^{13}C NMR (126 MHz, DMSO-d_6) δ 167.68, 161.96, 159.94, 153.46, 145.75, 137.32, 132.42, 131.78, 131.40, 130.04, 128.00, 127.69, 125.77, 125.40, 122.18, 122.07, 120.40, 116.56, 116.40, 106.60, 56.76, 55.97.ESI-MS: m/z387.0$[M - Br]^+$.

*1-(4-Fluorobenzyl)-4-(6-methoxy-2-naphthamido)pyridin-1-ium chloride (**4ad**).* Yield: 91%; white solid; m.p. 275–277 °C; IR(ν_{max}): 3625, 3584, 3418, 2356, 2092, 1658, 1650, 1643, 1633, 1518, 1481, 1459, 1396, 1326, 1157, 1071, 1046, 1027 cm^{-1}; ^{1}H NMR (400 MHz, DMSO-d_6) δ 12.01 (s, 1H), 8.88 (d, J = 7.1 Hz, 2H), 8.71 (s, 1H), 8.41 (d, J = 7.0 Hz, 2H), 7.96 (d, J = 8.6, 1.4 Hz, 1H), 7.89–7.82 (m, 2H), 7.50–7.47 (m, 2H), 7.31 (d, J = 2.0 Hz, 1H), 7.19–7.14 (m, 3H), 5.59 (s, 2H), 3.79 (s, 3H); ^{13}C NMR (126 MHz, DMSO-d_6) δ 167.70, 163.91, 161.96, 159.93, 153.53, 145.39, 137.30, 131.66, 131.59, 131.48, 131.44, 130.34, 127.87, 127.63, 127.57, 125.55, 120.29, 116.63, 116.49, 116.46, 106.55, 61.17, 55.95.ESI-MS: m/z387.0 $[M - Cl]^+$.

*1-(2-Nitrobenzyl)-4-(6-methoxy-2-naphthamido)pyridin-1-ium bromide (**4ae**).* Yield: 89%; white solid; m.p. 280–282 °C; IR (ν_{max}):

3385, 2391, 2351, 2304, 2318, 1703, 1643, 1621, 1588, 1520, 1485, 1329, 1282, 1269, 1245, 1214, 1192, 1167, 1078, 1043 cm^{-1}; ^1H NMR (400 MHz, DMSO-d_6) δ 11.76 (s, 1H), 8.82 (d, J = 4.8 Hz, 2H), 8.61 (s, 1H), 8.39 (d, J = 6.2 Hz, 2H), 8.26 (d, J = 8.1 Hz, 1H), 8.04 (d, J = 9.0 Hz, 1H), 8.01 (s, 2H), 7.84 (t, J = 7.6 Hz, 1H), 7.75 (t, J = 7.8 Hz, 1H), 7.46 (s, 1H), 7.32–7.27 (m, 2H), 6.05 (s, 2H), 3.92 (s, 3H); ^{13}C NMR (101 MHz, DMSO-d_6) δ 167.77, 160.01, 153.69, 148.11, 146.19, 137.41, 135.42, 131.44, 130.99, 130.09, 128.07, 127.69, 126.12, 125.45, 122.96, 120.43, 116.41, 106.70, 59.52, 56.02. ESI-MS: m/z414.0 $[M - Br]^+$.

*1-(4-Nitrobenzyl)-4-(6-methoxy-2-naphthamido)pyridin-1-ium bromide (**4af**).* Yield: 90%; white solid; m.p. 264–266 °C; IR(ν_{max}): 3020, 2919, 3030, 2851, 1669, 1624, 1439, 1328, 1215, 1116 cm^{-1}; ^1H NMR (400 MHz, DMSO-d_6) δ 11.68 (s, 1H), 8.93 (d, J = 7.2 Hz, 2H), 8.60 (s, 1H), 8.36 (d, J = 7.2 Hz, 2H), 8.23 (d, J = 8.7 Hz, 2H), 7.98–7.93 (m, 4H), 7.67 (d, J = 8.7 Hz, 2H), 7.39 (s, 1H), 7.23 (dd, J = 9.0, 2.3 Hz, 1H), 5.84 (s, 2H), 3.85 (s, 3H); ^{13}C NMR (126 MHz, DMSO-d_6) δ 167.71, 159.97, 153.55, 148.29, 145.94, 142.27, 137.35, 131.40, 130.24, 130.00, 128.03, 127.73, 127.63, 125.37, 124.64, 120.44, 116.53, 115.48, 106.62, 61.04, 55.98.ESI-MS: m/z414.0$[M - Br]^+$.

*1-Benzyl-4-((7-methoxy-2-naphthamido)methyl)pyridin-1-ium bromide (**4ag**).* Yield: 88%; brownish sticky-solid; IR (ν_{max}): 3850, 3743, 3301, 2920, 2850, 1628, 1602, 1540, 1503, 1483, 1390, 1415, 1301, 1266, 1216, 1165, 1020 cm^{-1}; ^1H NMR (400 MHz, MeOD) δ 8.98 (d, J = 6.7 Hz, 2H), 8.42 (s, 1H), 8.09 (d, J = 6.5 Hz, 2H), 7.92–7.90 (m, 4H), 7.49 (d, J = 2.1 Hz, 3H), 7.34 (d, J = 2.4 Hz, 1H), 7.25 (dd, J = 9.0, 2.5 Hz, 1H), 5.82 (s, 2H), 3.97 (s, 3H); ^{13}C NMR (126 MHz, MeOD) δ 169.24, 160.76, 159.61, 144.12, 136.88, 133.32, 130.25, 129.59, 129.31, 128.68, 127.96, 127.83, 127.75, 126.98, 126.17, 123.93, 119.55, 105.38, 63.74, 54.59, 42.63. ESI-MS: m/z383.0 $[M - Br]^+$.

*1-Benzyl-4-(2-(6-methoxy-2-naphthamido)ethyl)pyridin-1-ium bromide (**4ah**).* Yield 91%; brownish sticky solid; IR (ν_{max}): 3123, 3068, 3030, 2952, 2918, 2849, 2355, 1693, 1639, 1591, 1518, 1455, 1327, 1259, 1205, 1163, 1084 cm^{-1}; ^1H NMR (400 MHz, MeOD) δ 8.91 (d, J = 6.6 Hz, 2H), 8.22 (s, 1H), 8.06 (d, J = 6.6 Hz, 2H), 7.86–7.81 (m, 2H), 7.76–7.74 (m, 1H), 7.45 (s, 4H), 7.30 (d, J = 2.4 Hz, 1H), 7.22 (dd, J = 9.0, 2.5 Hz, 1H), 5.79 (s, 2H), 3.95 (s, 3H), 3.86 (t, J = 6.6 Hz, 2H); ^{13}C NMR (126 MHz, MeOD) δ 168.97, 161.35, 159.44, 143.69, 136.63, 133.41, 130.13, 129.50, 129.27, 128.71, 128.53, 127.92, 127.22, 126.84, 123.82, 119.42, 105.33, 63.63, 54.56, 39.02, 35.44. ESI-MS: m/z 397.0 $[M - Br]^+$.

*4-(2-(6-Methoxy-2-naphthamido)ethyl)-1-(2-methylbenzyl)pyridin-1-ium bromide (**4ai**).* Yield: 90%; white solid; m.p. 130–132 °C; IR (ν_{max}): 3583, 3388, 2955, 2925, 2351, 2322, 1729, 1640, 1536, 1502, 1390, 1301, 1216, 1164, 1025 cm^{-1}; ^1H NMR (400 MHz, MeOD) δ 8.84 (d, J = 6.6 Hz, 2H), 8.30 (s, 1H), 8.12 (d, J = 6.4 Hz, 2H), 7.92–7.84 (m, 3H), 7.83 (d, J = 8.6 Hz, 1H), 7.46–7.42 (m, 1H), 7.36 (s, 2H), 7.33–7.27 (m, 2H), 5.91 (s, 2H), 4.01 (s, 3H), 3.93 (t, J = 6.6 Hz, 2H), 2.34 (s, 3H); ^{13}C NMR (101 MHz, MeOD) δ 168.95, 161.43, 159.49, 143.69, 137.43, 136.67, 131.10, 130.15, 129.88, 129.76, 128.70, 128.55, 127.96, 127.25, 126.87, 126.80, 123.84, 119.46, 105.37, 61.77, 54.58, 39.03, 35.56, 17.82.ESI-MS: m/z411.0 $[M - Br]^+$.

*1-(2-Chlorobenzyl)-4-(2-(6-methoxy-2-naphthamido)ethyl)pyridin-1-ium chloride (**4aj**).* Yield: 91%; white solid; m.p. 173–175 °C; IR(ν_{max}): 3123, 3068, 3030, 2952, 2918, 2849, 2355, 1693, 1639, 1591, 1518, 1455, 1327, 1259, 1205, 1163, 1084 cm^{-1}; ^1H NMR (400 MHz, MeOD) δ 8.85 (d, J = 6.4 Hz, 2H), 8.21 (s, 1H), 8.05 (d, J = 6.3 Hz, 2H), 7.84–7.80 (m, 3H), 7.75 (d, J = 8.6 Hz, 2H), 7.55–7.44 (m, 4H), 5.91 (s, 2H), 3.93 (s, 3H), 3.85 (t, J = 6.5 Hz, 2H); ^{13}C NMR (101 MHz, MeOD) δ 161.72, 159.44, 143.92, 136.63, 134.31, 131.85, 131.62, 130.60, 130.21, 130.12, 128.60, 128.54, 127.97, 127.93, 127.22, 126.83, 123.81, 119.42, 105.34, 61.35, 54.55, 38.96, 35.48. ESI-MS: m/z431.0 $[M - Cl]^+$.

*1-(3-Chlorobenzyl)-4-(2-(6-methoxy-2-naphthamido)ethyl)pyridin-1-ium chloride (**4ak**).* Yield: 80%; white solid; m.p. 80–82 °C; IR (ν_{max}): 3374, 2955, 2924, 2853, 2356, 2327, 1744, 1641, 1536, 1462, 1377, 1302, 1274, 1214, 1191, 1160, 1026 cm^{-1}; ^1H NMR (400 MHz, MeOD) δ 8.99 (d, J = 6.5 Hz, 2H), 8.78 (s, 1H), 8.28 (s, 1H), 8.14 (d, J = 6.4 Hz, 2H), 7.92–7.88 (m, 2H), 7.81 (d, J = 8.5 Hz, 1H), 7.62 (s, 1H), 7.53–7.50 (m, 1H), 7.46 (t, J = 8.2 Hz, 1H), 7.36 (s, 1H), 7.28 (dd, J = 9.0, 2.3 Hz, 1H), 5.85 (s, 2H), 4.02 (s, 3H), 3.92–3.93 (m, 2H); ^{13}C NMR (126 MHz, MeOD) δ 168.99, 161.69, 159.46, 143.77, 136.64, 135.49, 135.00, 130.83, 130.11, 129.62, 128.82, 128.59, 128.51, 127.92, 127.19, 126.89, 126.85, 123.78, 119.46, 105.31, 62.75, 54.55, 39.02, 35.55. ESI-MS: m/z 431.0 $[M - Cl]^+$.

*1-(4-Chlorobenzyl)-4-(2-(6-methoxy-2-naphthamido)ethyl)pyridin-1-ium chloride (**4al**).* Yield: 93%; white solid; m.p. 115–116 °C; IR (ν_{max}): 3374, 2921, 2372, 2350, 2320, 1700, 1695, 1658, 1635, 1539,1533, 1516, 1456, 1216, 1162, 1029 cm^{-1}; ^1H NMR (400 MHz, MeOD) δ 8.78 (d, J = 6.4 Hz, 2H), 8.08 (s, 1H), 7.95 (d, J = 6.4 Hz, 2H), 7.74–7.70 (m, 2H), 7.61 (d, J = 8.6 Hz, 1H), 7.32 (s, 4H), 7.19 (d, J = 2.1 Hz, 1H), 7.11 (dd, J = 9.0, 2.4 Hz, 1H), 5.65 (s, 2H), 3.84 (s, 3H), 3.75 (t, J = 6.4 Hz, 2H); ^{13}C NMR (101 MHz, MeOD) δ 170.43, 163.05, 160.90, 145.11, 138.05, 137.00, 133.51, 131.57, 131.52, 130.77, 130.23, 129.95, 129.36, 128.59, 128.27, 125.17, 120.86, 106.84, 64.20, 56.00, 40.39, 36.96. ESI-MS:m/z 431.0 $[M - Cl]^+$.

*1-(2-Fluorobenzyl)-4-(2-(6-methoxy-2-naphthamido)ethyl)pyridin-1-ium bromide (**4am**).* Yield: 87%; white solid; m.p. 125–127 °C; IR (ν_{max}): 3414, 3048, 2923, 2849, 2356, 2327, 1824, 1767, 1756, 1746, 1729, 1712, 1700, 1679, 1658, 1652, 1641, 1635, 1565, 1533, 1495, 1456, 1393, 1302, 1276, 1161, 1026 cm^{-1}; ^1H NMR (400 MHz, MeOD) δ 8.78 (d, J = 6.3 Hz, 2H), 8.09 (s, 1H), 7.93 (d, J = 6.4 Hz, 2H), 7.69 (t, J = 9.0 Hz, 2H), 7.61 (d, J = 8.6 Hz, 1H), 7.47–7.38 (m, 2H), 7.18–7.14 (m, 2H), 7.08 (t, J = 8.8 Hz, 2H), 5.74 (s, 2H), 3.81 (s, 3H), 3.72 (t, J = 6.6 Hz, 2H); ^{13}C NMR (126 MHz, MeOD) δ 169.00, 161.66, 159.46, 143.83, 136.64, 132.35, 132.28, 131.23, 130.10, 128.70, 128.54, 127.92, 126.83, 125.18, 123.79, 120.52, 119.44, 115.92, 115.75, 105.30, 58.07, 54.53, 38.99, 35.48. ESI-MS: m/z 415.0 $[M - Br]^+$.

*1-(4-Fluorobenzyl)-4-(2-(6-methoxy-2-naphthamido)ethyl)pyridin-1-ium chloride (**4an**).* Yield: 95%; white solid; m.p. 120–122 °C; IR (ν_{max}): 3374, 2955, 2924, 2869, 2853, 2351, 2313, 1735, 1638, 1537, 1491, 1461, 1377, 1246, 1211, 1190, 1160, 1082 cm^{-1}; ^1H NMR (400 MHz, MeOD) δ 8.77 (d, J = 6.1 Hz, 2H), 8.08 (s, 1H), 7.92 (d, J = 6.0 Hz, 2H), 7.71–7.66 (m, 2H), 7.61 (d, J = 8.6 Hz, 1H), 7.41–7.37 (m, 2H), 7.15 (s, 1H), 7.04 (dd, J = 17.3, 8.8 Hz, 1H), 5.63 (s, 1H), 3.80 (s, 3H), 3.71 (t, J = 5.9 Hz, 2H); ^{13}C NMR (126 MHz, DMSO-d_6) δ 168.95, 164.47, 162.49, 161.43, 159.45, 143.63, 136.62, 131.06, 130.99, 130.12, 129.52, 128.74, 128.53, 127.92, 127.21, 126.83, 123.81, 119.44, 116.16, 115.98, 105.33, 62.76, 54.55, 39.01, 35.45.ESI-MS: m/z 415.0 $[M - Cl]^+$.

*4-(2-(6-Methoxy-2-naphthamido)ethyl)-1-(2-nitrobenzyl)pyridin-1-ium bromide (**4ao**).* Yield: 90%; white solid; m.p. 200–202 °C; IR (ν_{max}): 3584, 3564, 3361, 2920, 2371, 2355, 2319, 1844, 1767, 1734, 1729, 1700, 1695, 1690, 1684, 1667, 1652, 1635, 1554, 1539, 1331, 1213, 1029, 869, 814, 767, 732, 667, 631, 604, 595, 586, 577, 568, 559, 550, 532, 523, 515, 506 cm^{-1}; ^1H NMR (400 MHz, MeOD) δ 8.92 (d, J = 6.5 Hz, 2H), 8.38 (d, J = 8.2 Hz, 1H), 8.30 (s, 1H), 8.16 (d, J = 6.5 Hz, 2H), 7.93–7.88 (m, 3H), 7.85–7.81 (m, 2H), 7.51 (d, J = 7.5 Hz, 1H), 7.37 (d, J = 2.0 Hz, 1H), 7.28 (dd, J = 8.9, 2.4 Hz, 1H), 6.22 (s, 2H), 4.02 (s, 3H), 3.95 (dd, J = 12.0, 5.9 Hz, 2H); ^{13}C NMR (126 MHz, MeOD) δ 168.99, 161.87, 159.44, 147.95, 144.10, 136.63, 134.72, 131.93, 131.06, 130.14, 128.60, 127.93, 127.71, 127.26, 126.84, 125.82, 123.84, 119.43, 105.30, 60.79, 54.55, 39.04, 35.60.ESI-MS: m/z442.0 $[M - Br]^+$.

*4-(2-(7-Methoxy-2-naphthamido)ethyl)-1-(4-nitrobenzyl)pyridin-1-ium bromide (**4ap**).*Yield: 95%; white solid; m.p. 184–186 °C; IR (ν_{max}): 3417, 3338, 3273, 3046, 2921, 2849, 2351, 2327, 1767, 1729, 1712, 1700, 1695, 1684, 1680, 1634, 1620, 1565, 1554, 1518, 1481, 1468, 1453, 1426, 1382, 1346, 1320, 1289, 1260, 1243, 1216, 1156,

1116, 1016 cm^{-1};^{1}H NMR (400 MHz, DMSO-d_6) δ 9.06 (d, J = 5.7 Hz, 2H), 8.72 (t, J = 5.6 Hz, 1H), 8.26 (d, J = 6.0 Hz, 2H), 8.23 (s, 1H), 8.12 (d, J = 6.0 Hz, 2H), 7.88 (d, J = 9.0 Hz, 1H), 7.84 (d, J = 8.6 Hz, 1H), 7.78 (d, J = 8.6 Hz, 1H), 7.67 (d, J = 8.2 Hz, 2H), 7.36 (s, 1H), 7.22 (dd, J = 9.0 Hz, 1H), 5.95 (s, 2H), 3.89 (s, 3H), 3.72 (dd, J = 12.3, 6.2 Hz, 2H), 3.23 (t, J = 6.4 Hz, 2H); ^{13}C NMR (126 MHz, DMSO-d_6) δ 166.96, 161.63, 159.03, 148.28, 144.70, 141.96, 136.26, 130.82, 130.23, 129.58, 129.25, 127.85, 127.71, 127.13, 124.98, 124.59, 106.30, 61.92, 55.81, 39.19, 35.56.ESI-MS: *m/z*442.0 $[M - Br]^+$.

*1-Benzyl-4-(4-(benzyloxy)benzamido)pyridin-1-ium bromide (**4aq**).* Yield 91%, brown sticky solid; IR (ν_{max}): 3353, 2922, 2350, 2337, 2306, 1653, 1591, 1506, 1453, 1415, 1382, 1331, 1258, 1213, 1093, 1108 cm^{-1}; ^{1}H NMR (400 MHz, DMSO-d_6) δ 11.33 (s, 1H), 8.84 (d, J = 6.8 Hz, 2H), 8.22 (d, J = 6.8 Hz, 2H), 7.92 (d, J = 8.5 Hz, 2H), 7.35–7.19 (m, 10H), 7.08 (d, J = 8.5 Hz, 2H), 5.59 (s, 2H), 5.11 (s, 2H); ^{13}C NMR (126 MHz, DMSO-d_6) δ 166.84, 162.77, 153.34, 145.51, 136.88, 135.20, 131.17, 129.67, 129.61, 128.98, 128.52, 128.29, 125.36, 116.34, 115.35, 70.08, 62.06.ESI-MS: *m/z*395.0 $[M - Br]^+$.

*1-Benzyl-4-(4-phenoxybenzamido)pyridin-1-ium bromide (**4ar**).* Yield: 93%: white solid; m.p. 174–176 °C; IR (ν_{max}): 3393, 3066, 3027, 2925, 2318, 2351, 1962, 1693, 1639, 1606, 1588, 1518, 1504, 1488, 1455, 1375, 1326, 1286, 1242, 1206, 1161, 1118, 1081, 1043, 1022, 1010 cm^{-1};^{1}H NMR (400 MHz, MeOD) δ 8.81 (d, J = 7.4 Hz, 2H), 8.38 (d, J = 7.4 Hz, 2H), 8.07–8.05 (m, 2H), 7.51–7.44 (m, 6H), 7.26 (t, J = 7.4 Hz, 1H), 7.13–7.08 (m, 4H), 5.69 (s, 2H); ^{13}C NMR (101 MHz, DMSO-d_6) δ 166.84, 161.76, 155.42, 153.19, 145.52, 135.08, 131.43, 130.89, 129.70, 129.67, 128.97, 127.53, 125.35, 120.39, 117.82, 116.44, 62.19. ESI-MS: *m/z* 381.0 $[M - Br]^+$.

*1-Benzyl-4-(2-(4-(benzyloxy)phenyl)acetamido)pyridin-1-ium bromide (**4as**).* Yield: 89%; white solid; m.p. 187–189 °C; IR (ν_{max}): 3251, 3166, 3064, 3032, 3005, 2955, 2870, 2351, 2314, 1870, 1697, 1682, 1593, 1511, 1454, 1416, 1380, 1332, 1297, 1243, 1106, 1063, 1024, 1001 cm^{-1}; ^{1}H NMR (400 MHz, DMSO-d_6) δ 11.62 (s, 2H), 8.88 (d, J = 7.1 Hz, 2H), 8.10 (d, J = 7.1 Hz, 2H), 7.44 (t, J = 3.3 Hz, 7H), 7.39 (t, J = 7.4 Hz, 2H), 7.33 (t, J = 7.1 Hz, 1H), 7.25 (d, J = 8.5 Hz, 2H), 6.98 (d, J = 8.6 Hz, 2H), 5.68 (s, 2H), 5.10 (s, 2H), 3.76 (s, 2H); ^{13}C NMR (101 MHz, DMSO-d_6) δ 172.57, 157.85, 152.61, 145.77, 137.57, 135.15, 130.94, 129.65, 129.58, 128.91, 128.90, 128.26, 128.07, 126.81, 115.65, 115.24, 69.61, 62.07, 42.94.ESI-MS:*m/z*409.0 $[M - Br]^+$.

*4-([1,1′-Biphenyl]-4-ylcarboxamido)-1-benzylpyridin-1-ium bromide (**4at**).* Yield: 94%; white solid; m.p. 337–339 °C; IR(ν_{max}): 3418, 2954, 2924, 2350, 1691, 1639, 1586, 1518, 1503, 1461, 1416, 1202, 1171, 1125 cm^{-1}; ^{1}H NMR (400 MHz, DMSO-d_6) δ 11.63 (s, 1H), 8.97 (d, J = 6.9 Hz, 2H), 8.37 (d, J = 6.9 Hz, 2H), 8.14 (d, J = 8.1 Hz, 2H), 7.94 (d, J = 8.3 Hz, 2H), 7.80 (d, J = 7.8 Hz, 2H), 7.54 (t, J = 7.5 Hz, 2H), 7.50–7.44 (m, 6H), 5.73 (s, 2H); ^{13}C NMR (101 MHz, DMSO) δ 167.34, 153.16, 145.64, 145.17, 139.13, 135.15, 131.97, 129.69, 129.62, 128.99, 127.52, 127.37, 116.54, 62.20. ESI-MS:*m/z* 365.0 $[M - Br]^+$.

*1-Ethyl-4-(6-methoxy-2-naphthamido)pyridin-1-ium iodide (**4au**).* Yield: 85%; white solid; m.p. 241–243 °C; IR (ν_{max}): 3301, 2955, 2924, 2869, 2852, 2357, 2337, 1735, 1695, 1625, 1590, 1518, 1461, 1377, 1325, 1272, 1205, 1190, 1159, 1124, 1026 cm^{-1}; ^{1}H NMR (400 MHz, DMSO-d_6) δ 11.62 (s, 1H), 8.89 (d, J = 7.1 Hz, 2H), 8.63 (s, 1H), 8.34 (d, J = 7.1 Hz, 2H), 8.06 (d, J = 9.0 Hz, 1H), 8.02 (s, 2H), 7.48 (d, J = 2.2 Hz, 1H), 7.33 (dd, J = 9.0, 2.4 Hz, 1H), 4.50 (q, J = 7.3 Hz, 2H), 3.95 (s, 3H), 1.53 (t, J = 7.3 Hz, 3H); ^{13}C NMR (101 MHz, DMSO-d_6) δ 167.70, 159.92, 152.82, 145.19, 137.29, 131.38, 129.77, 128.16, 127.76, 127.63, 125.31, 120.43, 116.18, 106.60, 55.98, 55.17, 16.48. ESI-MS: *m/z* 307.0 $[M - I]^+$.

***In vitro* AChE and BChE inhibition assay.** In vitro cholinesterase inhibitory assay was performed following Ellman assay protocol [35,48,49]. *Electrophorus electricus* acetylcholinesterase (EeAChE, EC 3.1.1.7, from electric eel, Type V–S, 827 U/mg solid; 1256 U/mg of protein), and butyrylcholinesterase (EqBChE, E.C. 3.1.1.8, from equine serum, 246 U mg/solid, 855 U/mg protein) were used for cholinesterase inhibition studies. Enzymes and substrates were diluted using 0.1 M phosphate buffer pH: 7.2 (PBS) to get the desired stocks. 10 mM stock solutions of compounds were prepared using biological grade DMSO and diluted with PBS to get the desired final concentration. All experiments were carried out in 96 well plates. The assay solution consists of 20 μL enzyme solution (AChE or BChE), 20 μL test compound solution and 140 μL 0.3 mM 5,5-dithiobis-(2-nitrobenzoic acid) solution (DTNB). This assay mixture was incubated for 20 min at 37 °C followed by addition of 20 μL 10 mM substrate (acetyl thiocholine iodide or *S*-butyryl thiocholine iodide). Immediately after addition of the substrate, the reaction was monitored by recording the absorbance at 412 nm every minute for 10 min using a 96-well microplate plate reader. Donepezil was used as reference standard and each concentration was assayed in triplicate. Finally, percent inhibition and IC_{50} values were determined. The detailed protocol has been described earlier [30].

Enzyme kinetics. The kinetic studies of compound **7b** with rHuAChE and eqBChE was carried out using the same protocol as described above. For each concentration of **7b,** five different concentrations of substrate were used. The procedure of kinetic experiment for K_i determination is described earlier in our previous paper [30].

***In vitro* PAMPA-BBB assay**. The test compound was dissolved in DMSO (10 mM stock), and was further diluted with PBS to get 100 μM stock. The 0.2 ml of each test compounds and PBS were added to the donor and acceptor plates, respectively. The absorbance of both plates was recorded using microplate reader, and the effective permeability was calculated as described earlier [36].

Aβ42 self-aggregation inhibition assay. Amyloid beta 1–42 rat peptide (Sigma-Aldrich, Saint Louis) was pretreated with 10% (w/v) NH_4OH (0.5 mg/ml) in order to produce an aggregate free solution. After brief sonication and incubation for 10 min at room temperature, NH_4OH was removed using vacuum concentrator resulting in a fluffy white peptide [50]. The obtained peptide was reconstituted in a mixture of CH_3CN/0.3 mM Na_2CO_3/250 mM NaOH (48.4:48.4:3.2) to obtain a 200 μM solution. Assays were carried out in 96-well black microtiter plates at a final assay volume of 200 μL with final Aβ and inhibitor concentrations of 20 and 10 μM, respectively. Incubation of Aβ with and without inhibitors were carried out for 24 h at 30 °C in 10 mM phosphate buffer (pH = 8.0) containing 10 mM NaCl. All the assays were carried out in duplicate. Quantification of aggregates of Aβ was done using Thioflavin T (ThT) fluorescence method. ThT (final concentration of 40 μM) was added to the assay solutions after incubation and fluorescence intensity was recorded for 300 s with an interval of 30 s (λexc = 446 nm; λem = 490 nm) [51]. Background signal was recorded in blank wells containing only tested inhibitors and ThT. The percentage inhibition due to the presence of test compound was calculated by the following expression: 100 - ($IF_i/IF_o \times 100$), where IF_i and IF_o are the respective fluorescence intensities obtained in the presence and in the absence of inhibitor, respectively.

Molecular modeling. The docking studies were carried in the same way as described earlier [30]. Briefly, the crystal structures of human AChE (PDB ID: 4EY7) and human BChE (PDB ID: 6EP4) were retrieved from RCSB-PDB and the proteins were prepared, minimized, optimized and grids were generated in Schrodinger program. The ligand **7b** was sketched in ChemDraw and prepared using Ligprep module of Schrodinger program. Finally docking was carried out using XP glide docking module of Schrodinger program.

The PV file retrieved from XP docking of protein–ligand docked complex was used for the MD simulation studies. The protein-ligand complex was solvated and neutralized under default setting of Desmond program. The ligand–protein complex was minimized by steepest descent method followed by the BFGS

(Broyden– Fletcher–Goldfarb–Shanno) algorithm. Further, MD simulation studies were carried under default conditions over a period of 10ns. Desmond software (v3.8) was used for MD simulation studies. The complete protocol is described our previous publication [52].

Author contributions

The manuscript was written through the contributions of all authors. All authors have approved the final version of the paper. M. Abdullaha performed the synthesis of compounds and docking studies; VKN performed biological evaluations; SBB designed, and coordinated all this work. SBB wrote the manuscript. IIIM Publication number. CSIR-IIIM/IPR/00214

Interest statement

Authors do not have any conflict of interest.

Declaration of competing interest

The authors declare that they have no known competing financial interests or personal relationships that could have appeared to influence the work reported in this paper.

Acknowledgement

M. Abdullaha thanks UGC for the research fellowship. The financial support from the CSIR YSA grant (P90807) is gratefully acknowledged.

Abbreviations

AD	Alzheimer's disease
AChE	acetylcholinesterase
ACh	acetyl choline
BBB	Blood Brain Barrier
ACN	acetonitrile
CAS	catalytic anionic site
CIs	cholinesterase inhibitors
DMF	dimethyl formamide
DMSO	dimethyl sulphoxide
EeAChE	acetylcholinesterase from Electrophorus *electricus* (electric eel)
eqBChE	Equine serum butyrylcholinesterase
k_m	Michaelis-Menten constant
Ki	inhibition constant
PAS	peripheral anionic site
PDB	protein data bank
rHuAChE	recombinant human acetylcholinesterase
SEM	standard error of mean

Appendix A. Supplementary data

Supplementary data to this article can be found online at https://doi.org/10.1016/j.ejmech.2020.112761.

References

[1] World Alzheimer Report, 2019: Attitudes to Dementia, Alzheimer's Disease International (ADI), London, 2019. Published by.
[2] M. Goedert, M.G. Spillantini, A century of Alzheimer's disease, Science 314 (5800) (2006) 777–781.
[3] J. Wang, B.J. Gu, C.L. Masters, Y.J. Wang, A systemic view of Alzheimer disease - insights from amyloid-β metabolism beyond the brain, Nat. Rev. Neurol. 13 (11) (2017) 703.
[4] S. Haider, S. Saleem, T. Perveen, S. Tabassum, Z. Batool, S. Sadir, et al., Age-related learning and memory deficits in rats: role of altered brain neurotransmitters, acetylcholinesterase activity and changes in antioxidant defense system, Age (Dordr) 36 (3) (2014) 9653.
[5] C.Y. Shin, H.S. Kim, K.H. Cha, D.H. Won, J.Y. Lee, S.W. Jang, et al., The effects of donepezil, an acetylcholinesterase inhibitor, on impaired learning and memory in rodents, Biomol Ther (Seoul) 26 (3) (2018) 274–281.
[6] A. Chatonnet, O. Lockridge, Comparison of butyrylcholinesterase and acetylcholinesterase, Biochem. J. 260 (3) (1989) 625–634.
[7] M.B. Colovic, D.Z. Krstic, T.D. Lazarevic-Pasti, A.M. Bondzic, V.M. Vasic, Acetylcholinesterase inhibitors: pharmacology and toxicology, Curr. Neuropharmacol. 11 (3) (2013) 315–335.
[8] R.M. Lane, S.G. Potkin, A. Enz, Targeting acetylcholinesterase and butyrylcholinesterase in dementia, Int. J. Neuropsychopharmacol. 9 (1) (2006) 101–124.
[9] P. Taylor, Z. Radić, The cholinesterases: from genes to proteins, Annu. Rev. Pharmacol. Toxicol. 34 (1994) 281–320.
[10] H. Dvir, I. Silman, M. Harel, T.L. Rosenberry, J.L. Sussman, Acetylcholinesterase: from 3D structure to function, Chem. Biol. Interact. 187 (1–3) (2010) 10–22.
[11] J.L. Sussman, M. Harel, I. Silman, Three-dimensional structure of acetylcholinesterase and of its complexes with anticholinesterase drugs, Chem. Biol. Interact. 87 (1–3) (1993) 187–197.
[12] N.C. Inestrosa, A. Alvarez, C.A. Pérez, R.D. Moreno, M. Vicente, C. Linker, et al., Acetylcholinesterase accelerates assembly of amyloid-beta-peptides into Alzheimer's fibrils: possible role of the peripheral site of the enzyme, Neuron 16 (4) (1996) 881–891.
[13] D.J. Selkoe, Translating cell biology into therapeutic advances in Alzheimer's disease, Nature 399 (6738 Suppl) (1999) A23–A31.
[14] Y.J. Huang, Y. Huang, H. Baldassarre, B. Wang, A. Lazaris, M. Leduc, et al., Recombinant human butyrylcholinesterase from milk of transgenic animals to protect against organophosphate poisoning, Proc. Natl. Acad. Sci. U. S. A. 104 (34) (2007) 13603–13608.
[15] C.I. Wright, C. Geula, M.M. Mesulam, Neurological cholinesterases in the normal brain and in Alzheimer's disease: relationship to plaques, tangles, and patterns of selective vulnerability, Ann. Neurol. 34 (3) (1993) 373–384.
[16] M.M. Mesulam, A. Guillozet, P. Shaw, A. Levey, E.G. Duysen, O. Lockridge, Acetylcholinesterase knockouts establish central cholinergic pathways and can use butyrylcholinesterase to hydrolyze acetylcholine, Neuroscience 110 (4) (2002) 627–639.
[17] N.H. Greig, T. Utsuki, Q. Yu, X. Zhu, H.W. Holloway, T. Perry, et al., A new therapeutic target in Alzheimer's disease treatment: attention to butyrylcholinesterase, Curr. Med. Res. Opin. 17 (3) (2001) 159–165.
[18] E.K. Perry, R.H. Perry, G. Blessed, B.E. Tomlinson, Changes in brain cholinesterases in senile dementia of Alzheimer type, Neuropathol. Appl. Neurobiol. 4 (4) (1978) 273–277.
[19] T. Darreh-Shori, O. Almkvist, Z.Z. Guan, A. Garlind, B. Strandberg, A.L. Svensson, et al., Sustained cholinesterase inhibition in AD patients receiving rivastigmine for 12 months, Neurology 59 (4) (2002) 563–572.
[20] E. Giacobini, R. Spiegel, A. Enz, A.E. Veroff, N.R. Cutler, Inhibition of acetyl- and butyryl-cholinesterase in the cerebrospinal fluid of patients with Alzheimer's disease by rivastigmine: correlation with cognitive benefit, J. Neural. Transm. 109 (7–8) (2002) 1053–1065.
[21] C. Holmes, C. Ballard, D. Lehmann, A. David Smith, H. Beaumont, I.N. Day, et al., Rate of progression of cognitive decline in Alzheimer's disease: effect of butyrylcholinesterase K gene variation, J. Neurol. Neurosurg. Psychiatry 76 (5) (2005) 640–643.
[22] M. Mesulam, A. Guillozet, P. Shaw, B. Quinn, Widely spread butyrylcholinesterase can hydrolyze acetylcholine in the normal and Alzheimer brain, Neurobiol. Dis. 9 (1) (2002) 88–93.
[23] H. Akincioglu, I. Gulcin, Potent acetylcholinesterase inhibitors: potential drugs for Alzheimer's disease, Mini Rev. Med. Chem. 20 (8) (2020) 703–715.
[24] P. Anand, B. Singh, A review on cholinesterase inhibitors for Alzheimer's disease, Arch Pharm. Res. (Seoul) 36 (4) (2013) 375–399.
[25] T. Artunc, A. Menzek, P. Taslimi, I. Gulcin, C. Kazaz, E. Sahin, Synthesis and antioxidant activities of phenol derivatives from 1,6-bis(dimethoxyphenyl) hexane-1,6-dione, Bioorg. Chem. 100 (2020) 103884.
[26] E. Bursal, P. Taslimi, A.C. Goren, I. Gulcin, Assessments of anticholinergic, antidiabetic, antioxidant activities and phenolic content of *Stachys annua*, Biocat. Agric. Biotechnol. 28 (2020) 101711.
[27] Z.Q. Cheng, K.K. Zhu, J. Zhang, J.L. Song, L.A. Muehlmann, C.S. Jiang, et al., Molecular-docking-guided design and synthesis of new IAA-tacrine hybrids as multifunctional AChE/BChE inhibitors, Bioorg. Chem. 83 (2019) 277–288.
[28] H.R. Liu, C. Zhou, H.Q. Fan, J.J. Tang, L.B. Liu, X.H. Gao, et al., Novel potent and selective acetylcholinesterase inhibitors as potential drugs for the treatment of Alzheimer's disease: synthesis, pharmacological evaluation, and molecular modeling of amino-alkyl-substituted fluoro-chalcones derivatives, Chem. Biol. Drug Des. 86 (4) (2015) 517–522.
[29] V.K. Nuthakki, R. Mudududdla, A. Sharma, A. Kumar, S.B. Bharate, Synthesis and biological evaluation of indoloquinoline alkaloid cryptolepine and its bromo-derivative as dual cholinesterase inhibitors, Bioorg. Chem. 90 (2019) 103062.
[30] V.K. Nuthakki, A. Sharma, A. Kumar, S.B. Bharate, Identification of embelin, a 3-undecyl-1,4-benzoquinone from Embelia ribes as a multitargeted anti-Alzheimer agent, Drug Dev. Res. 80 (5) (2019) 655–665.
[31] K. Sharma, Cholinesterase inhibitors as Alzheimer's therapeutics (Review),

Mol. Med. Rep. 20 (2) (2019) 1479–1487.
[32] J. Wu, M. Pistolozzi, S. Liu, W. Tan, Design, synthesis and biological evaluation of novel carbamates as potential inhibitors of acetylcholinesterase and butyrylcholinesterase, Bioorg. Med. Chem. 28 (5) (2020) 115324.
[33] G. Joshi, S. Kalra, U.P. Yadav, P. Sharma, P.K. Singh, S. Amrutkar, et al., E-pharmacophore guided discovery of pyrazolo[1,5-c]quinazolines as dual inhibitors of topoisomerase-I and histone deacetylase, Bioorg. Chem. 94 (2020) 103409.
[34] A. Kumar, E. Rathi, S.G. Kini, E-pharmacophore modelling, virtual screening, molecular dynamics simulations and in-silico ADME analysis for identification of potential E6 inhibitors against cervical cancer, J. Mol. Struct. 1189 (2019) 299–306.
[35] G.L. Ellman, K.D. Courtney, V. Andres, R.M. Featherstone, A new and rapid colorimetric determination of acetylcholinesterase activity, Biochem. Pharmacol. 7 (2) (1961) 88–95.
[36] N. Augustin, V.K. Nuthakki, M. Abdullaha, Q.P. Hassan, S.G. Gandhi, S.B. Bharate, Discovery of Helminthosporin, an Anthraquinone isolated from rumex abyssinicus Jacq as a dual cholinesterase inhibitor, ACS Omega 5 (3) (2020) 1616–1624.
[37] F. Li, Z.M. Wang, J.J. Wu, J. Wang, S.S. Xie, J.S. Lan, et al., Synthesis and pharmacological evaluation of donepezil-based agents as new cholinesterase/monoamine oxidase inhibitors for the potential application against Alzheimer's disease, J. Enzym. Inhib. Med. Chem. 31 (sup3) (2016) 41–53.
[38] J. Cheung, M.J. Rudolph, F. Burshteyn, M.S. Cassidy, E.N. Gary, J. Love, et al., Structures of human acetylcholinesterase in complex with pharmacologically important ligands, J. Med. Chem. 55 (22) (2012) 10282–10286.
[39] T.L. Rosenberry, X. Brazzolotto, I.R. Macdonald, M. Wandhammer, M. Trovaslet-Leroy, S. Darvesh, et al., Comparison of the binding of reversible inhibitors to human butyrylcholinesterase and acetylcholinesterase: a crystallographic, kinetic and calorimetric study, Molecules 22 (12) (2017).
[40] M. Abdullaha, S. Mohammed, M. Ali, A. Kumar, R.A. Vishwakarma, S.B. Bharate, Discovery of quinazolin-4(3H)-ones as NLRP3 inflammasome inhibitors: computational design, metal-free synthesis, and in vitro biological evaluation, J. Org. Chem. 84 (9) (2019) 5129–5140.
[41] S. Wangngae, C. Duangkamol, M. Pattarawarapan, W. Phakhodee, Significance of reagent addition sequence in the amidation of carboxylic acids mediated by PPh3 and I2, RSC Adv. 5 (33) (2015) 25789–25793.
[42] M. Navarro, C.A. Smith, M. Albrecht, Enhanced catalytic activity of iridium(III) complexes by facile modification of C,N-bidentate chelating pyridylideneamide ligands, Inorg. Chem. 56 (19) (2017) 11688–11701.
[43] S. Hassan, S.A. Ejaz, A. Saeed, M. Shehzad, S. Ullah Khan, J. Lecka, et al., 4-Aminopyridine based amide derivatives as dual inhibitors of tissue non-specific alkaline phosphatase and ecto-5′-nucleotidase with potential anticancer activity, Bioorg. Chem. 76 (2018) 237–248.
[44] J.L. Vrijdag, F. Delgado, N. Alonso, W.M. De Borggraeve, N. Pérez-Macias, J. Alcázar, Practical preparation of challenging amides from non-nucleophilic amines and esters under flow conditions, Chem. Commun. 50 (95) (2014) 15094–15097.
[45] J. Liang, V. Tsui, A. Van Abbema, L. Bao, K. Barrett, M. Beresini, et al., Lead identification of novel and selective TYK2 inhibitors, Eur. J. Med. Chem. 67 (2013) 175–187.
[46] J.L. Archibald, P. Fairbrother, J.L. Jackson, Benzamidopiperidines. 3. Carbocyclic derivatives related to indoramin, J. Med. Chem. 17 (7) (1974) 739–745.
[47] J.L. Archibald, P. Fairbrother, J.L. Jackson, Benzamidopiperidines. 3. Carbocyclic derivatives related to indoramin, J. Med. Chem. 17 (7) (1974) 739–745.
[48] K. Cetin Cakmak, I. Gulcin, Anticholinergic and antioxidant activities of usnic acid-an activity-structure insight, Toxicol Rep 6 (2019) 1273–1280.
[49] Taslimi P, Gulçin İ. Antioxidant and anticholinergic properties of olivetol. J. Food Biochem.42: e12516.
[50] T.M. Ryan, J. Caine, H.D. Mertens, N. Kirby, J. Nigro, K. Breheney, et al., Ammonium hydroxide treatment of Aβ produces an aggregate free solution suitable for biophysical and cell culture characterization, Peer J. 1 (2013) e73.
[51] M. Bartolini, C. Bertucci, M.L. Bolognesi, A. Cavalli, C. Melchiorre, V. Andrisano, Insight into the kinetic of amyloid beta (1-42) peptide self-aggregation: elucidation of inhibitors' mechanism of action, Chembiochem 8 (17) (2007) 2152–2161.
[52] P. Joshi, G.J.P. McCann, V.R. Sonawane, R.A. Vishwakarma, B. Chaudhuri, S.B. Bharate, Identification of potent and selective CYP1A1 inhibitors via combined ligand and structure-based virtual screening and their in vitro validation in sacchrosomes and live human cells, J. Chem. Inf. Model. 57 (6) (2017) 1309–1320.